Numerical and Experimental Analysis of Dual Focus Laser for High Aspect Ratio Microdrilling

Jasjit Singh Mann

A Thesis

In

The Department

Of

Mechanical and Industrial Engineering

Presented In Partial Fulfillment of the Requirement

For the Degree of Master of Applied Science (Mechanical Engineering) at

Concordia University

Montreal, Quebec, Canada

December, 2008

Library and Archives
Canada

Published Heritage
Branch

395 Wellington Street
Ottawa ON K1A 0N4
Canada

Bibliothèque et
Archives Canada

Direction du
Patrimoine de l'édition

395, rue Wellington
Ottawa ON K1A 0N4
Canada

Canada

ABSTRACT

Numerical and experimental analysis of dual focus laser for high aspect ratio microdrilling

Jasjit Singh Mann

Laser drilling is the most efficient noncontact material removal process. In this research project, a simplified approach using "dual focus" has been proposed to improve the aspect ratio of the drilling. Dual focus drilling not only changes the kerf angle but also increases the depth of drilling due to redistribution of the intensity in the overlapping focusing region. The dual focus is achieved by focusing two wavelengths at two different foci along the optical axis, using a single lens. A theoretical study of dual beam propagation along the optical axis was done for the selection of the radius of curvature of the lens to achieve continuity within the two focusing regions to increase the aspect ratio. Modeling has been done with numerical approach to understand the impact of intensity distribution and optical parameters on the efficiency of dual wavelength drilling.

Objective of the research work is to optimize the laser as well as optical parameters theoretically as well as experimentally with respect to dual wavelength drilling for obtaining high aspect ratio drilled holes with minimum power. The microdrilling station was setup with second harmonic generation to achieve dual wavelength with maximum

conversion efficiency of 20%. Experiments were done individually with laser wavelengths of 532nm and 1064nm and with focusing both these wavelengths using a single lens at different pulse energies, on 500μm thick silicon wafers. SEM observation of results proved that dual frequency drilling is more efficient compared to conventional drilling and results show excellent agreement with the results from the theoretical model.

ACKNOWLEDGEMENTS

Table of Contents

List of figures

List of tables

Chapter 1 Introduction

1.1 Introduction

From its early life as "an invention looking for a job"(Harry Stine) the laser has been successfully used in the electrical, mechanical, industrial, biomedical and aerospace industry. The first major industrial use of laser was the drilling of holes in diamond wire drawing dies in the 1960's [1]. The high reproducibility and precision of the laser drilling process make it attractive to industry where it is being used to form small diameter and high aspect ratio holes in a wide variety of materials. Moreover, Laser drilling has an additional advantage of noncontact drilling which reduce surface damage.

Laser drilling has ability to drill holes in hard material such as superalloys, ceramics, and composites without the high rate of tool wear normally associated with conventional machining. Conventional mechanical drilling is slow process and associated with difficulties to drill at high angles [2]. In laser drilling, material removal take place either by melt ejection or by vaporization. The laser drilling of composites materials such as multilayer carbon fiber composites for aircraft application is attracting interest due to potential advantages of rapid processing, ability to drill high-aspect ratio at low kerf angles and without tool wear [3]. Laser is well suited for the nonconducting and metallic substrates coated with nonconducting materials where the electric discharge machining is limited. For example, the drilling of thermal barrier-coated super alloys in aerospace

1

application can be well achieved by laser drilling instead of electrical discharge machining [4]. Review of literature suggests different methods of micro drilling based on different requirements that vary depending upon the drill dimensions, material properties as well as the applications. These methods can be broadly classified as laser based and non laser based technologies with lots of processes variations to suit particular applications. The different methods of micro drilling are shown below in fig 1.1. As there are different methods, of micro drilling each has its own advantage and disadvantage over the others which are discussed in the subsequent sections.
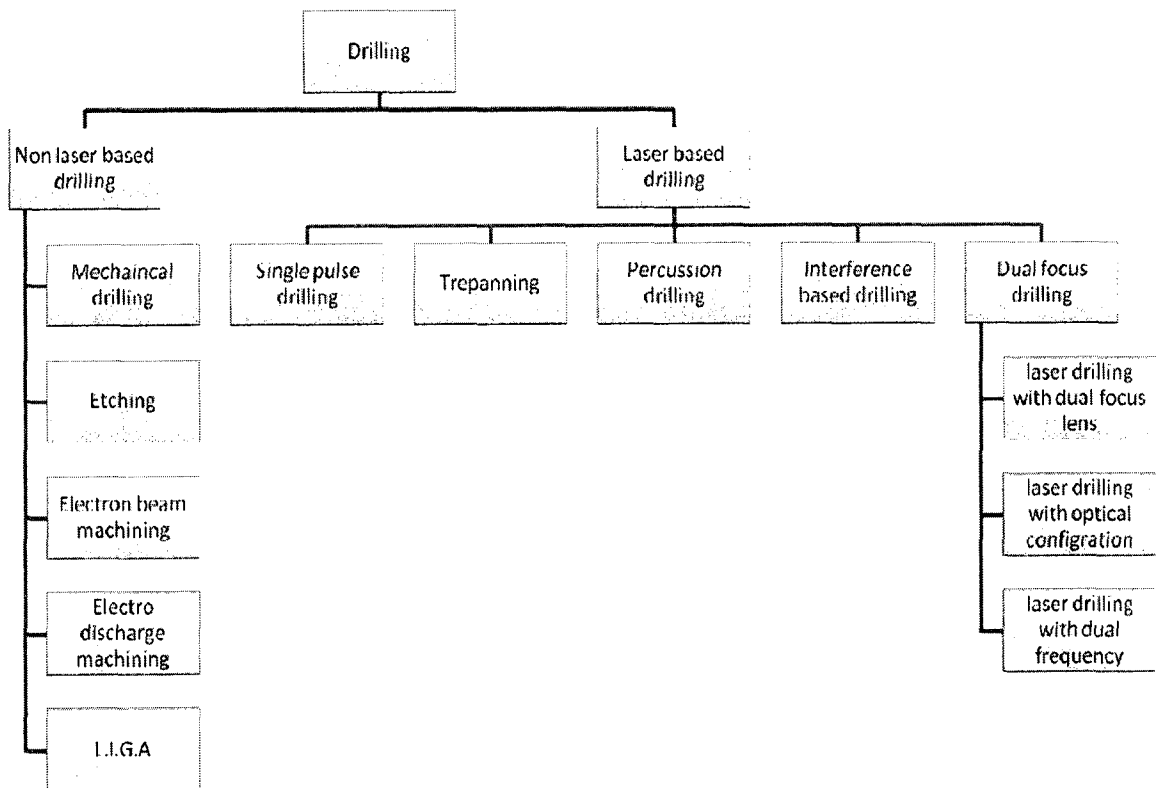
Fig 1.1 *Different methods of drilling [5-15].*

1.2 Drilling with non laser based technology

1.2.1 Mechanical drilling

The micro drilling is process of using a drill tool to produce cylindrical holes in solid material. Different tools are used for drilling different types of materials. The hole is drilled precisely with reference to the x, y, and z-axes. Thought in mechanical drilling holes are produced with good roundness, straightness and surface quality in a short machining time, it is not suitable for micro drilling. Micro drilling refers to the drilling holes less than ϕ 0.5 mm. Microdrilling at this small diameter presents greater problems since it requires tools of very small diameter, high precision machine with high spindle speeds. Moreover, the process limits the aspect ratio due to the large length to diameter ratio which causes the drill bit to deflect which can cause misalignment or tool breakage. In the mechanical micro drilling of brittle materials, cracks are generated at the exit surfaces [5]. Mechanical drilling is not versatile process for example change of holes dimension require change of drill bits as well as feed rate and spindle speed. To overcome this limitation of mechanical microdrilling, there are non conventional methods that are discussed henceforth.

1.2.2 Etching

Etching is a process of using strong acid to cut into the unprotected parts of a metal surface to create a design in the metal. In general, there are two classes of etching; wet etching and dry etching. Wet Etching is a process that utilizes liquid chemicals or

3

etchants to remove materials, usually in specific patterns defined by photoresist masks. Materials not covered by masks are etched away by chemicals while those covered by the masks are left intact. Wet etching is generally isotropic as shown in fig 1.2, i.e., it proceeds in all directions at same rate. Anisotropic etchings, in contrast to isotropic etching, means different etch rates in different directions in the material [6].

Material

Mask

Anisotropic   **Isotropic**
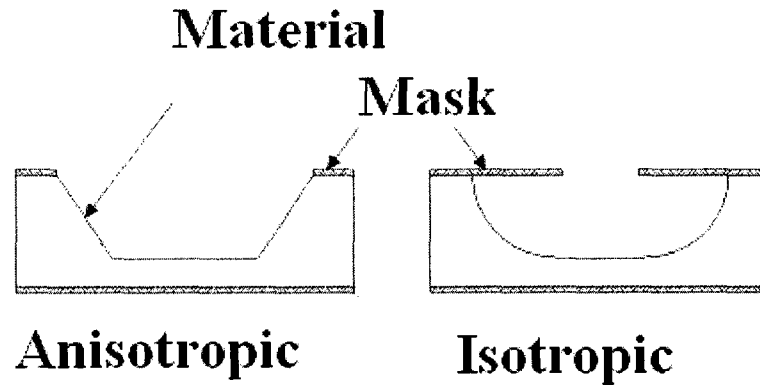
Fig 1.2 *Etching process*

Dry etching is a process that utilizes only dry chemicals or etchants to remove material. Dry etching technology can be split into three separate classes; 1) chemical dry etching; 2) sputtering and reactive ion etching; 3) combination of chemical, sputtering and reactive ion etching [7]. Material removal rate is high in dry etching as compared to wet etching. Moreover etching process requires mask that make the process complicated and time consuming. Moreover when new dimensions are needed, a new mask design is required, reducing the versatility of this technique.

4

1.2.3 Electron beam machining

Electron-beam machining (EBM) is a machining process where high-velocity electrons are directed toward a work piece, creating heat and vaporizing the material as shown in fig 1.3. EBM machines utilize voltages in the range of 50 to 200 kV to accelerate electrons to 200,000 km/s. Electromagnetic lenses are used to direct the electron beam, by means of deflection, into a vacuum [8]. The electrons strike the top layer of the work piece, removing material, and then get trapped in some layers beneath the surface. The requirement of hard vacuum to reduce contamination and to minimize electron collisions with air molecules, EBM is best suited for small parts.
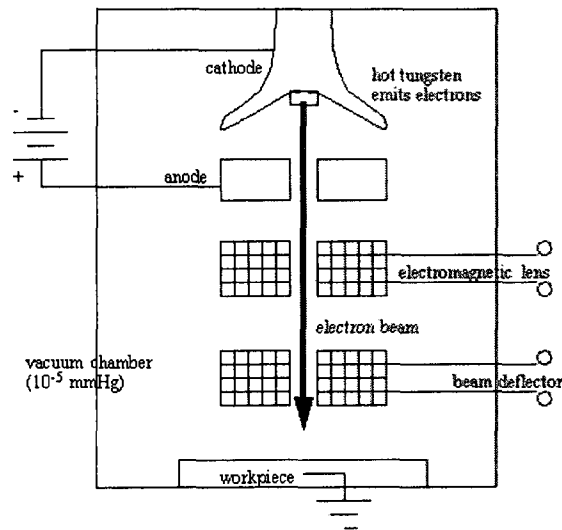
Fig 1.3 *Electron beam machining process [8]*

1.2.4 Electro discharge machining

Electro discharge machining (EDM) is a spark erosion process used to create complex shapes in electrically conductive work pieces. A thin wire 50 - 300μm in diameter with an aspect ratio of up to 300:1 is used as an electrode. A DC power supply delivers high frequency pulses to the electrode and work piece. The gap between the electrode and the work piece is flooded with deionized water, which acts as a dielectric medium and the material is machined by spark discharges. Though multiple electrodes can be used to drill holes, productivity is relatively low, the capital cost is high and recast layer is formed [9 - 12].

In electrochemical machining (ECM) process, metal is removed by a chemical reaction rather than the electrical action of the EDM arc. The work piece is positive anode of an electrochemical cell. The tool is cathode, which is normally formed in an inverse of the shape to be produced. The cathode and the work piece are brought together in a high pressure circulation of salt solution electrolyte in a DC electrode cell. In electrochemical drilling (ECD) the chemical drill is used. The drill is a conducting cylinder with an insulating coating on the outside. The electrolyte is pumped down through the centre of the tube. The tool is moved towards the work piece, and material at the base of the electrode of removed. Since the outer surface of the tool is insulated, the surface of the hole is not machined by the process [13]. The ECM is a well established process in the aviation industry for the production of turbine blades and for placement of cooling air bore holes. The process of ECM enables the machining of metal independent of their

6

mechanical properties with high material removal rates. As compare to EDM process the tool-electrode wear is extremely low and the sub-surface is not damaged. But with ECM sharp corners are not possible and work piece material must be homogeneous.

1.2.5 L.I.G.A.

LIGA is a German acronym for "Lithograghie, Galvanoformung, Abformung," in English (X-ray) Lithography, Electroforming, and Molding [14]. LIGA is one of the major techniques to allow on demand manufacturing of high aspect ratio structures with lateral precision below one micrometer. One of the defining features of LIGA is the use of ultraviolet light sources that have shorter wavelength and higher resolution, which is important in the fabrication of MEMS devices.

Fig 1.4 shows the steps in LIGA process. The first step is to deposit a thick layer of photo resist on the substrate [14]. X-rays bombard the photo resist layer, creating precise micro-cavities in the shape of the parts that are desired. In the next step, the developed photo resist is used as a mould for electroforming. The components are created by electrodeposition, with the material filled in the gaps in the photo resist mould. The resist is then stripped, leaving behind the metal structure, which can be used either directly or as a mould for further processing [16]. However, some disadvantages of LIGA-process strongly limit itself in the industrial applications like the use of expensive X-ray source, availability of useful photo resists, process complications, time consumed to manufacture X-ray mask, and the possibility of only simple-geometry microstructures.
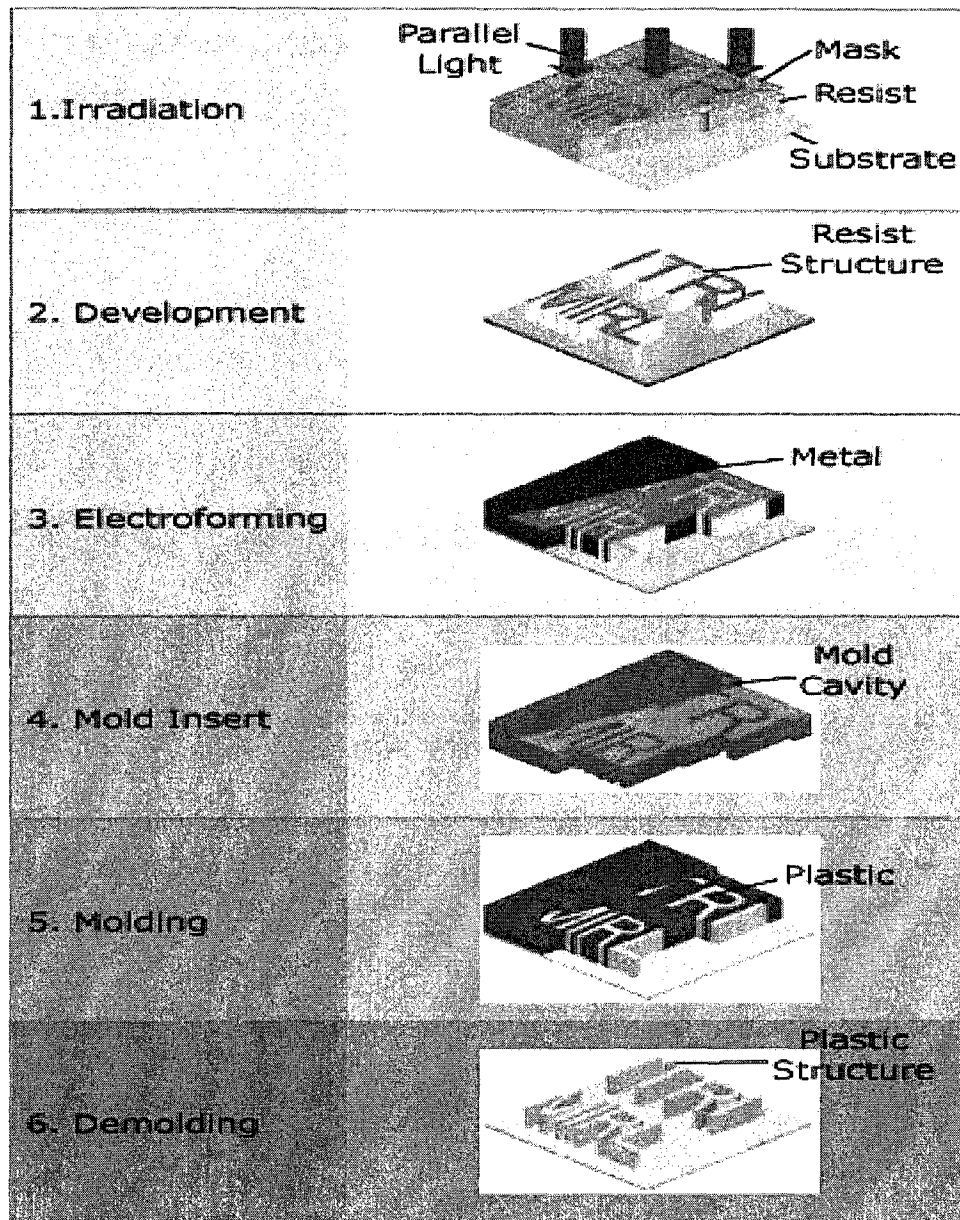
Fig 1.4 *Steps followed in L.I.G.A [15]*

As discussed above, non laser based drilling methods are characterized by the following

limitations. Mechanical drilling and electro chemical drilling processes have high tool

wear, and are difficult to drill hard materials such as super alloys. In case of etching, masks are needed that reduces the versatilities while in EBM hard vacuum is needed limiting the work piece size. LIGA is complicated requiring highly skilled operates and time consuming. Being a high energy density process laser based micro drilling overcome most of these limitations. The developments in laser based drilling are discussed in next section.

1.3 Drilling with laser based technology

Laser is basically a light source. The radiation that it emits is not fundamentally different than any other form of electromagnetic radiation. Laser has some unique properties having, high monochromaticity, high degree of coherence and brightness. In addition laser has energy tune ability and can be easily focused to a diffraction limited spot size.

1.3.1 Laser drilling

Laser drilling is a process in which the beam is stationary with respect to the work piece. The aim is to produce a cavity with high aspect ratio, which is primarily achieved by three methods: direct drilling, percussion drilling and trepanning. Laser machining is normally performed in air by focusing the laser beam onto the work piece. An assist gas is used principally to increase material removal rate using the melt shearing mechanism. In laser drilling material properties also play role to decide the laser parameters like

absorption relative to wavelength, latent heat, and ablation threshold value etc [17]. Laser drilling is carried out by using continuous wave mode or pulsed laser mode.

Continuous wave

A continuous wave (CW) is an electromagnetic wave of constant amplitude and frequency; and in mathematical analysis, of infinite duration. Fig 1.5 shows power distribution with respect to time, in case of CW laser the 't' in fig 1.5 is infinite and the laser power is constant with respect to time. Long pulse lasers having pulse widths of the order of few microseconds also fall under this category. Although continuous wave operation offers the advantages of smooth surfaces after machining the material removal is primarily due to melting and it is associated with high amount of heat generation. Due to which it is mostly used for industrial purposes where change in material properties are not critical. The laser damage threshold for continuous lasers is more difficult to measure.
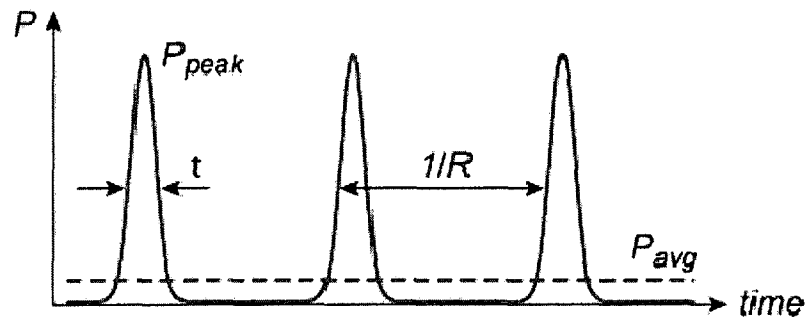
Fig 1.5 *Temporal mode of laser power [18]*

Pulsed laser

In pulsed laser the output of a laser varies with respect to time as shown in fig 1.5. Where t is pulse duration and P_{peak} is peak power of pulse. Peak pulse can be increased by reducing pulse width or by increasing repetition rate. Pulsed laser micromachining is based on the interaction of laser light with the material. Focused beam interacts with the work piece for small interval of time depending on the pulse width. Pulsed laser has lesser or no heat affected zone. Material removal process in pulsed laser micromachining can be divided in two categories; pyrolithic (thermal) and photolithic [19-22]. In pyrolithic process, material is removed by heating, melting and partial evaporation of the heated volume of the material. Nanosecond and microsecond pulsed lasers work on pyrolithic process. In photolithic process the proton energy of pulsed laser is sufficient to break the chemical bonds and aid material removal [22]. Picosecond and femtosecond lasers fall under this category of material removal. A figurative material removal mechanism of different lasers and their effects on the work piece is shown is fig 1.6.
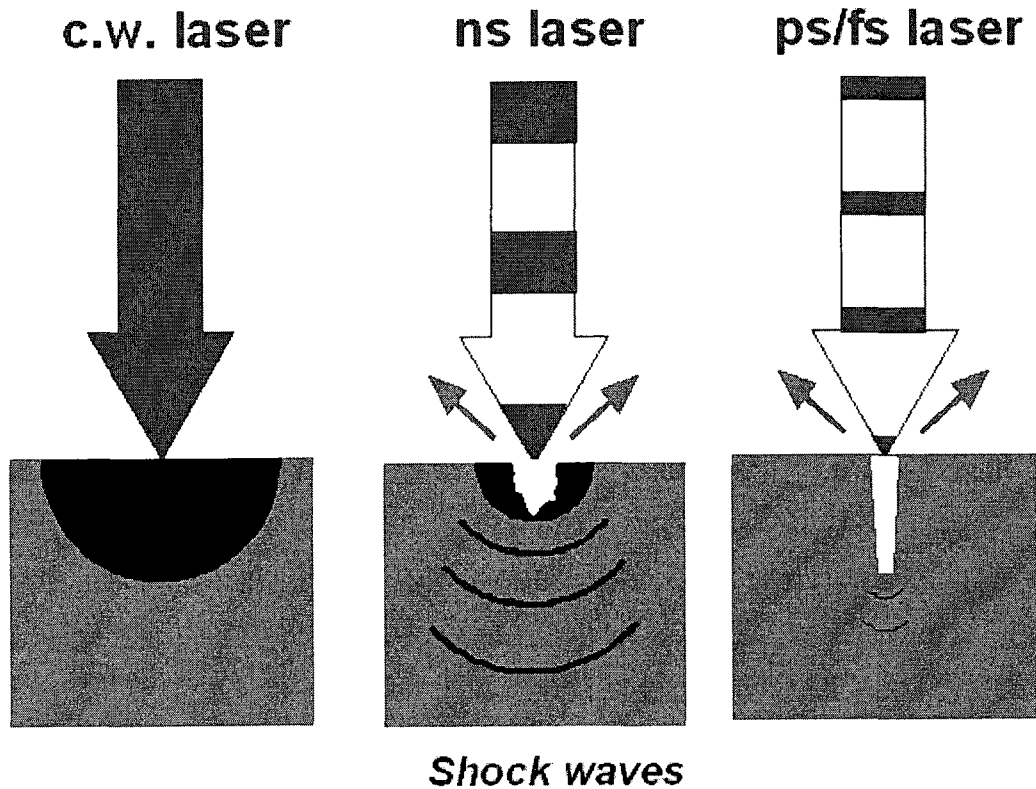
Fig 1.6 *Laser ablation mechanism [23]*

1.3.2 Ultra short pulse laser machining

Femtosecond pulsed lasers are ultrafast pulsed lasers. In femtosecond laser the fluence of the laser beam can be tightly controlled in such a way that sub spot size features can be machined that is why it is mostly used in research work related to surface patterning and sub micron machining [19, 24, and 25]. As mentioned in the previous section femtosecond pulsed laser works on photolithic process of material removal. Principle behind the material processing with femtosecond pulsed laser is multi-photon absorption. This does not depend on the presence of free electrons on the work piece therefore most

of the material including glass can be processed with femtosecond lasers. Machining with femtosecond lasers has no heat affected zone due to thermal diffusion time between two electrons is in the range of pico seconds which is larger than the pulse width. The ablation depth per pulse in femtosecond pulsed laser is given by equation 1.1

$$Z_a \approx \alpha^{-1} \, Ln \, [F_a/F_{th}] \qquad\qquad (1.1)$$

Where Z_a is the ablation depth, F_a is the absorbed fluence; F_{th} is the threshold fluence and α is the ablation depth [26-28]. Femtosecond laser are still not common in industries due to their high down time, low average energy and high initial cost.

A picosecond laser is a laser that emits pulse in the regime of pico seconds. The thermal diffusion time between two electrons is approx 10 ps range due to which heat transfer is almost negligible during material processing with picosecond lasers. In contradiction to femtosecond pulsed lasers where no liquid phase exists during material processing, picosecond laser have a liquid phase [29]. The ablation depth per pulse in picosecond is same as femtosecond pulsed lasers.

1.3.3 Short pulse laser machining

Nanosecond pulsed laser works on pyrolithic process of material removal, therefore heat affect zone is associated with nanosecond pulsed lasers. The ablation per pulse is given by equation 1.2

$$Z_a \approx \sqrt{(at)} \, Ln \, [F_a/F_{th}] \qquad\qquad (1.2)$$

Where Z_a is the ablation depth, F_a is the absorbed fluence, F_{th} is the threshold fluence, and $(a.t)$ is the thermal diffusion depth [[29-34]. The material removal mechanism is discussed in the following section.

1.3.4. Mechanisms of material removal

Material removal mechanisms during laser drilling are vaporization and the physical expulsion of the melt. Hole drilled with purely evaporative material removal mechanisms are generally marked with clean surface and sharp boundaries without recast layer, spatter. Material removal by melt expulsion is an energetically efficient mechanism. Generally, the energy required to remove the material via melt expulsion is about one quarter of that required to vaporize the same volume [35-36]. However the material removal by melt expulsion is generally irregular and may result in asymmetric and irregular holes shapes. When a laser beam of intensity is irradiated on the surface of material, it results in the excitation of free electrons in metals, vibrations in insulators, or both in semiconductors. This excitation energy is rapidly converted into heat which is followed by various heat transfer processes such as conduction into the materials, and convection and radiation from the surface. The most significant heat transfer process being the heat conduction into the material. The generation of heat at the surface and its conduction into the material establishes the temperature distribution in the material depending on the thermo-physical properties of the material and laser parameters. If the

incident laser intensity is sufficiently high, the absorption of the laser energy can result in the phase transformations such as surface melting and evaporation. Generally these phase transformations are associated with threshold laser intensities referred to as melting and evaporation thresholds.

The depth of melting cannot increase to infinitely large value with increasing laser energy density and pulse time because the location of the melting point in the temperature and depth is limited by the maximum achievable surface temperature. Once the surface temperature reaches the boiling point, the depth of melting reaches the maximum value. Further increase in the laser energy density or the pulse time cause the evaporative material removal from the surface without further increase in the depth of melting. So different drilling techniques have been devised to increase the aspect ratio, which are discussed below.

1.4 Techniques of laser drilling

In laser drilling the high intensity laser beam is focused onto the surface to heat, melt and subsequently eject the material in both liquid and vapor phases. In general there are three approaches of laser drilling; single pulse, trepanning, and percussion drilling are shown in fig.1.7. Where t is thickness of work piece and d is diameter of hole.

1.4.1 Single pulse drilling

Single pulse drilling is used for drilling less than $\phi 1mm$ holes through thin plates. High pulse energies are supplied in drilling with single pulse because the irradiated energy levels must be sufficient to vaporize the material in single pulse.

(a) Single pulse   (b) Trepanning   (c) Percussion
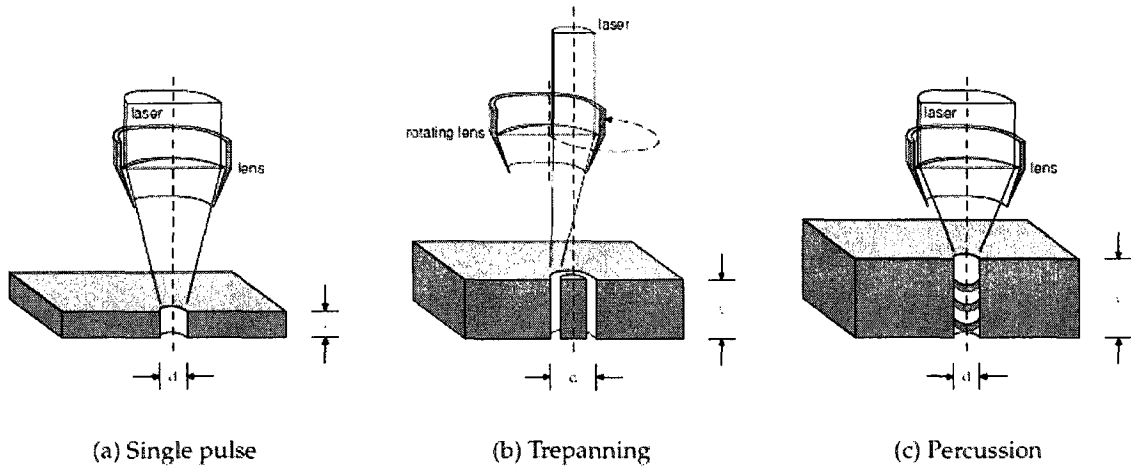
Fig 1.7 *Various techniques in laser drilling [37]*

1.4.2 Trepanning drilling

In trepanning wider holes less than 3mm in thicker plates are produced by drilling a series of overlapping holes around a circumference of a circle so as to cut a contour out of the plate. Trepanning can be performed by translating either the work piece or the focusing optic. The process similar to contour cutting and can be performed by the laser operating in the continuous wave or pulsed mode. CO_2 and Nd: YAG lasers are most commonly used in trepanning. Trepanning drilling requires a motion system to allow

16

piercing with the laser and then motion of the beam relative to the part to cut out the hole. Trepanning allows for a diameter tolerance that about half that of percussion drilling. Holes drilled in metals are judged by the hole diameter tolerance, taper, recast thickness, and micro cracking. Hole diameter in percussion drilled holes is generally less than +/- 50μm and in trepanned holes the tolerance tightens to about +/- 25μm. Recast is molten metal that resolidified around the hole's inner diameter and recast thickness varies with the material and hole depth but is generally held to less than 100μm. Hole depth can be as high a 50mm but most drilling tasks will have hole depths of less than 15mm.

1.4.3 Percussion laser drilling

In percussion drilling a series of short pulses (10^{-12} to 10^{-3}s) separated by longer time periods (10^{-2}s) are directed on the same spot to form a through hole. Each laser pulse contributes to the formation of the hole by removing a certain volume of the material [38]. Pulsed Nd: YAG laser are most commonly used for percussion drilling because of their higher energy per pulse. Percussion drilling is used to produce narrow holes (less than 1.3mm) through relatively thicker (up to 25mm) metals plates [39]. The parameters and number of pulses are chosen to produce a good quality hole. Holes in the 25μm to 1000μm diameter range can be drilled using this method but the limits vary according to the material to be drilled and the thickness. Most percussion drilled holes are in the 300μm-600μm diameter range. Percussion drilling can take advantage of pulse-shaping to improve the interaction of the laser beam with the material and help control taper and

improve drilling speed. Pulse shaping is programming the laser's pulse temporal profile. By breaking up a long drilling pulse into two three or four shorter segments separated by off-time the hole quality can be improved and speed increased. Debris coming out of the hole can interfere with end of a long duration pulse so breaking it up improves efficiency and reduces drilling time.

1.5 Interference based laser micro-drilling

In this method interference principle is used to form fringes. When two or more light waves of the same frequency overlap at a point, the resultant effect depends on the phases of the waves as well as their amplitudes. The resultant wave at any point at any instant of time is governed by the principle of superposition [40]. The combined effect at each point of the region of superposition is obtained by adding algebraically the amplitudes of the individual waves.
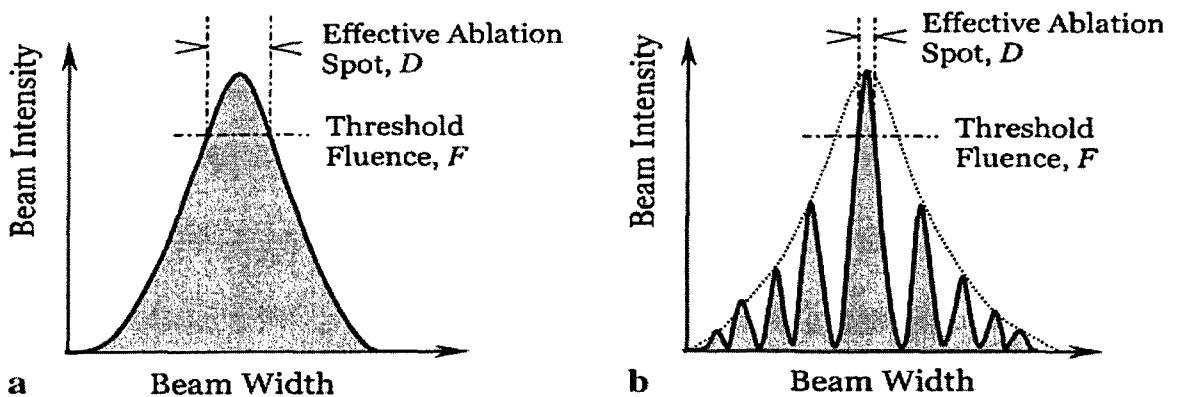
Fig 1.8 a) 2D profile of the conventional non-interfered Gaussian laser beam. b) 2D profile of the interfered Gaussian laser beam [41].

18

At certain points, the two waves are in phase, where the amplitude of the resultant wave (A_R) is equal to the amplitudes of the two waves, hence, the intensity of the resultant wave is given by equation 1.3

$$I_R \infty A_R{}^2 = 2^2 A^2 = 2^2 I \tag{1.3}$$

The interference produced at this point is known as constructive inference. If the two waves are in opposite phase, then the resultant intensity is less than the sum of the intensities due to individual waves and point is known as destructive interference [40]. The intensity distribution due to interference principle is shown in fig 1.8. In interference laser micromachining the intensity distribution varies along the fringes, intensity distribution is high at centre and reduces outward. Only those fringes in which intensity is higher than the threshold fluence of the material will contribute to machining. By this method, machining depends upon fringe width which cannot be less than wavelength of the light. Moreover the depth is limited for drilling, because if the energy is increased, other fringes start contributing in machining and increase heat affect zone. To avoid this dual focus laser drilling offer significant advantages to increase the intensity distribution along the depth, the research and development on dual focus micro drilling over the last few years are discussed in next section.

19

1.6 Dual focus laser micro-drilling.

Dual focus laser drilling is newly developed high aspect ratio drilling technique that has two focal points from a single laser source. Having two focal points, the intensity distribution at focus is increased along the depth of the focus which increases the drilling depth significantly without increasing the feature size. The different method of dual-focus drilling has been available in literature which is discussed below.

1.6.1 Dual focus laser drilling with dual focus lens

The first method of dual focus laser drilling is dual focus lens which was invented by S. E. Nielsen. The central portion of laser beam passes through centre of the lens, which has a longer focal length than the outer part of the lens as shown in the fig 1.9. Dual focus lens has two radii of curvature on one side, at centre of lens high radius curvature as compare to the remaining portion [42].
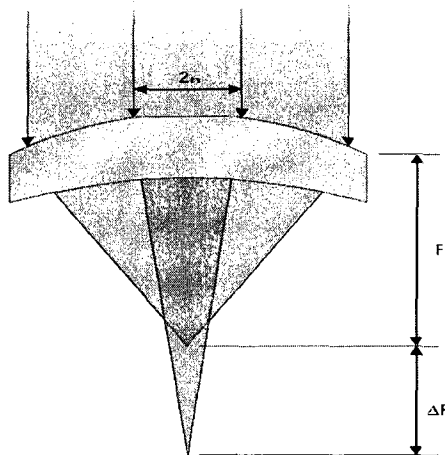
Fig 1.9 *Dual focus lens [42]*

20

Due to this, the beam is focused at two focal points. The shorter focal length is set near to the top surface of the work piece, and longer focal length set at the bottom surface of the work piece. The difference between two foci is ΔF as shown in fig 1.9. though dual focus lens improves the material removal rate and machining quality, but machining is restricted to macro size due to its large spot size (greater than a few hundred microns) and wide distance between two foci (over 1mm) [43]. Presently it's only used for CO_2 laser cutting. ΔF can only be changed by changing the lens, which is expensive. To overcome this there is other methods of dual focus generation by optical configuration.

1.6.2 Dual focus laser drilling with optical configuration

Laser drilling using dual focal point from single laser source, as discussed above by using dual focus lens, improves processing speed, and kerf quality. But it also has some disadvantages as macro spot size, and wide distance between two foci. B. Tan et al describe an optical configuration to generate the dual-focus from single laser source. A collimated laser beam is incident on a modified Newton's ring setup, which consists of a polarization plate beam splitter and a convex mirror [43] as shown in fig 1.10.

21
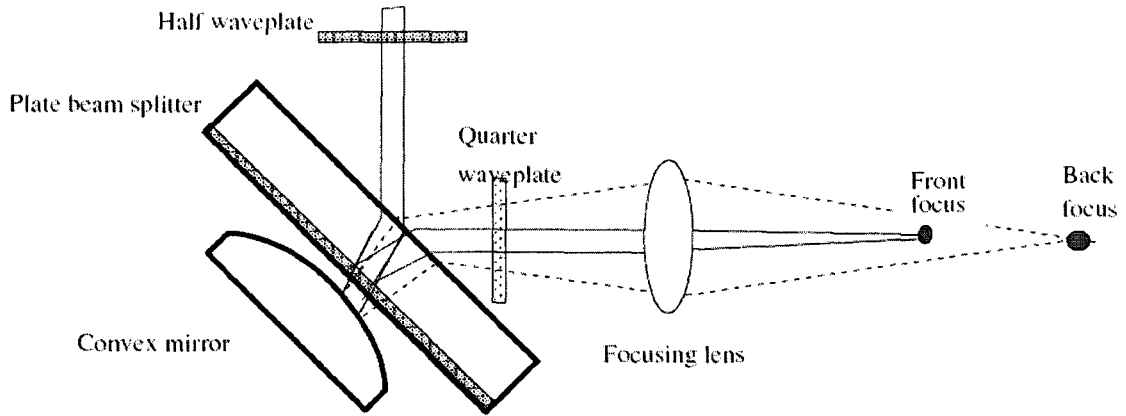
Fig 1.10 *Optical configuration to generate the dual focus [43]*

Laser beam is made to impinge on the optical configuration, the beam deflected from the beam splitter is collimated (dark line in fig 1.10) and the output beam which is reflected from the mirror is divergent (dashed line in fig 1.10) has divergent angle Θ given by

$$\Theta = D/R \qquad\qquad (1.4)$$

Where D is the diameter of the incident beam, and R is the radius of curvature of the convex mirror. After passing through the focusing lens, the beam focuses at two points; beam deflected from beam splitter is focused at designed focal length of the lens and diverged beam from the convex mirror focuses far from focal length of the lens. Rear spot size is large when compare to front spot size. Distance between two foci is adjusted by changing the radius of curvature of convex mirror or by changing laser beam diameter. Polarization coating on the rear side of the beam splitter and AR coating on its front side helps in arrangement of predetermined laser intensity ratio between the two

spots by varying the polarization using the half waveplate. In this method wavelength specific equipment is required, which restrict this setup to one specific wavelength. To avoid this, other method of dual focus drilling with dual wavelength is discussed in next section.

1.6.3 Dual focus laser machining with dual frequency beam

Second harmonic crystal is used to generate the dual frequency from single source. The emitted laser beam is guided to harmonic crystal, which double the optical frequency [44]. The energy ratio of the two frequencies is depends upon the transmission efficiency of the crystal. After traversing the harmonic crystal a dual frequency collimated beam is obtained. B. Tan et al develop this method with femtosecond laser to drill the thick PMMA plate. Due to different wavelength, the reflective index of the focusing medium is also different. So they focus at two different points in the same optical axis. Smaller wavelength will focus first and higher wavelength focuses after smaller wavelength as shown in fig.1.11.

Dual frequency
collimated beam

Focal
point
Smaller
wavelength

Focal point
Longer
wavelength

Plano-convex lens

dd
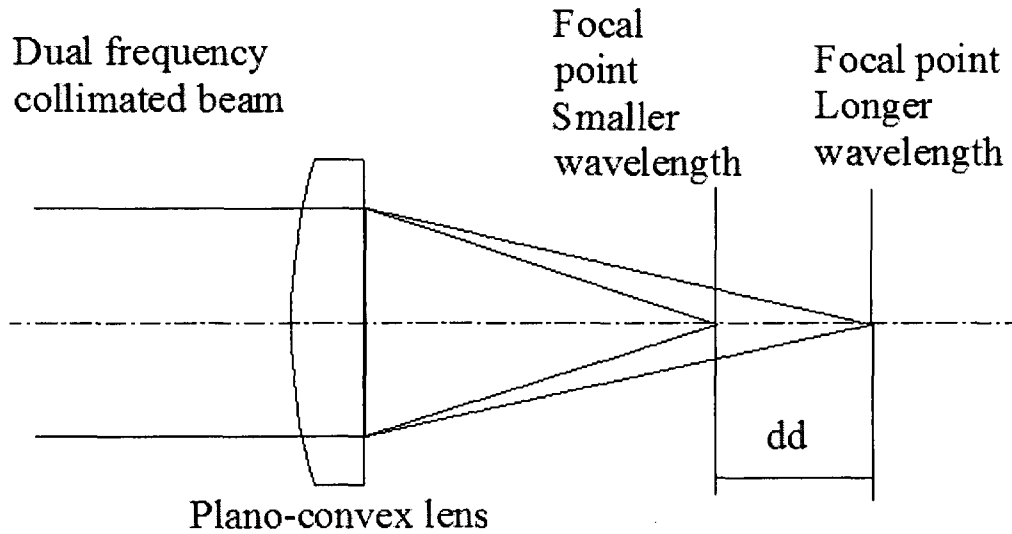
Fig 1.11 *Dual focus based on longitudinal achromatic aberration*

For this method, different wavelength combination can be used by changing the harmonic crystal. They also conclude that at the same drill depth the focus of dual frequency beam reduces the diameter of opening. Consequently, the aspect ratio is increased. Advantage of dual frequency laser drilling is the ability to choose the energy ratio according to absorption properties of the material with respect to the wavelength, by which drilling can be done with minimum power.

1.7 Problem definition

Due to increasing demand to miniaturize, there is a need for micro drilling with high aspect ratio from various industrial sectors like microelectronic, biomedical, aerospace

etc. Comprehensive review of literature suggests various mechanisms for microdrilling that are characterized with relative advantages and disadvantages. Like high tool wear, and difficult to drill hard material or super alloy, mask limits the versatility and work piece size limitation due to vacuum chamber, process complication requires highly skilled operates and time consuming. Being a high energy density process laser based micro drilling overcome most of these limitations.

1.8 Objective and scope of the work

High aspect laser drilling with dual frequency nanosecond pulsed laser with minimum power. The scope of the thesis include

1. Theoretical study of single and dual frequency micromachining and comparing the effect of power to understand the minimum requirement to induce maximum drilling depth

2. Theoretical analysis of the effect of radius of curvature of the plano convex lens on achieving continuity in dual frequency microdrilling

3. Setting up of the experimental system including the second harmonic generation (S.H.G) to perform dual frequency microdrilling

4. Study the effect of efficiency of S.H.G on microdrilling parameters

5. Perform microdrilling on 500μm thick silicon wafers with single and dual frequencies and optimizing the power of the laser for achieving maximum drill depth at high aspect ratio.

25

Chapter 2 Theoretical modeling

2.1 Introduction

Theoretical modeling has been done to predict and compare the drilling with single as well as with dual wavelength drilling with respect to different laser and optical parameters. Dual wavelength drilling has been proposed for high aspect ratio drilling with lower kerf angle. Principle of achromatic aberration has been used in the proposed project to focus two wavelengths at two different foci with a common focusing lens. Numerical modeling has been done with the help of MATLAB to study the high aspect ratio dual frequency drilling on silicon wafers at minimum possible power with respect to different laser as well as optical parameters.

2.2 Intensity distribution of single wavelength

All theoretical modeling have been done by considering single focusing lens with high transmissivity at the given wavelengths. The minimum focused spot radius 'w' and the depth of focus 'dof' which defines a working range for laser machining depends upon the focal length (fl), wavelength (λ) and unfocused beam diameter (d). For TEM_{oo} mode the following relationships are applicable [17].

$$w = 1.22 * \lambda * fl / d \qquad (2.1)$$

$$dof = 2.44 * \lambda * fl^2 / d^2 \qquad (2.2)$$

26
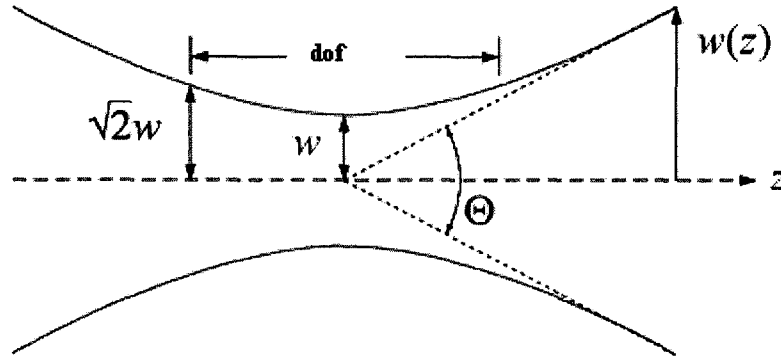
Fig 2.1 *Single beam focusing characteristics [65]*

From the equation 2.1 & 2.2 it could be understood that by increasing the focal length, the depth of focus can be increased; however, the spot diameter also increases, which ultimately reduces the energy density or intensity of the laser beam. For laser micromachining, it is good to use the shorter focal length in order to obtain minimum feature size and high laser intensity per unit area. The spot diameter can be decreased to reduce the feature size either by decreasing the focal length or by increasing the unfocused beam diameter. But increase in unfocused beam diameter also decreases the depth of focus which ultimately affects the aspect ratio of the drilling. As shown in fig 2.1 spot diameter varies due to which the energy density also varies along the z axis. Energy density above the material damage threshold helps in machining and energy density below the material damage threshold only contributing towards heating the material. Theoretically, depth of focus is considered as the length up to which machining can be done with minimum laser power above threshold fluence. After the Rayleigh range, which is defined as depth of focus, the laser beam diverges sharply. Divergent

27

nature of laser beam reduces the laser intensity drastically and the machining will stop due to higher threshold fluence in comparison to available intensity.
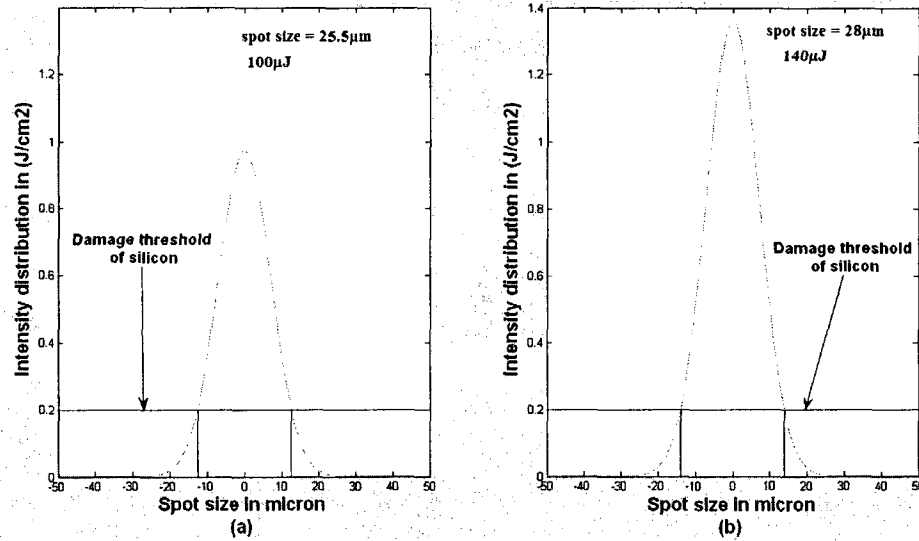
Fig 2.2 *Intensity distribution of 532nm at surface of the silicon wafer*

Fig 2.2 shows the intensity distribution at the surface of silicon wafer of laser beam of 532nm wavelength having beam diameter 1.6mm and focused with a lens of 12.9mm radius of curvature. Solid black line along the x-axis is damage threshold value of silicon and vertical straight lines at the interface shows the spot size on basis of intensity above the damage threshold value of silicon. In this fig 'w' is kept constant in both cases only pulse power is varied, (a) pulse energy is 100 μJ and (b) pulse energy is 140 μJ of 532nm wavelength. From this fig it can observed that with increase in pulse energy spot size also increases. This is due to per unit area intensity is increased which help in machining. As

discussed above, spot size varies along the 'z' due which per unit area intensity varies which varies the spot size.

2.3 Dual wavelength beam focusing

The objective of the research project is to design a drilling technique which employs chromatic aberration to focus two different wavelengths at two different depths in drilling to obtain high aspect ratio drilling. Chromatic aberration is caused due to lens having different refractive indices for different wavelengths of light, which focuses the different wavelengths at different foci. In dual focus drilling, it is important to consider the design of the lens in such a way that depth of focus of both the wavelengths makes continuity with each other. Different parameters play their role in continuity like beam diameter, wavelength of laser beam, radius of curvature, and refractive index of the lens material. The refractive index of lens material BK7 with respect to different wavelengths is shown in fig 2.3
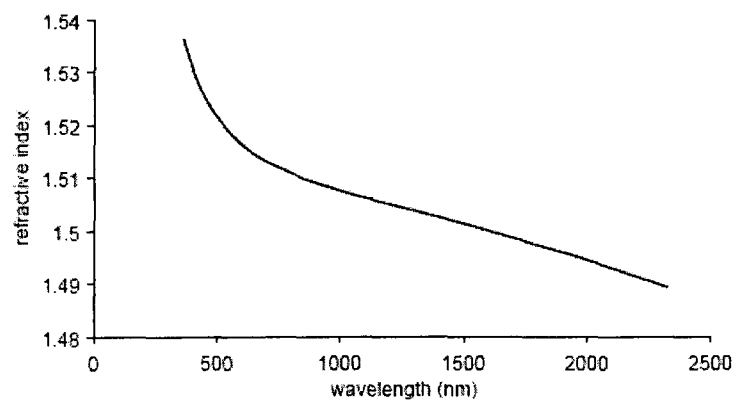
Fig 2.3 *Refractive index of BK7 material [48]*

29

As shown in fig 2.3 refractive index of BK7 reduces as the wavelength increases. Effect of refractive index on the focal length of different wavelengths is used to focus the dual wavelength at two different foci on same axis. Fig.2.4 shows the two different foci of dual wavelength with Plano convex lens.
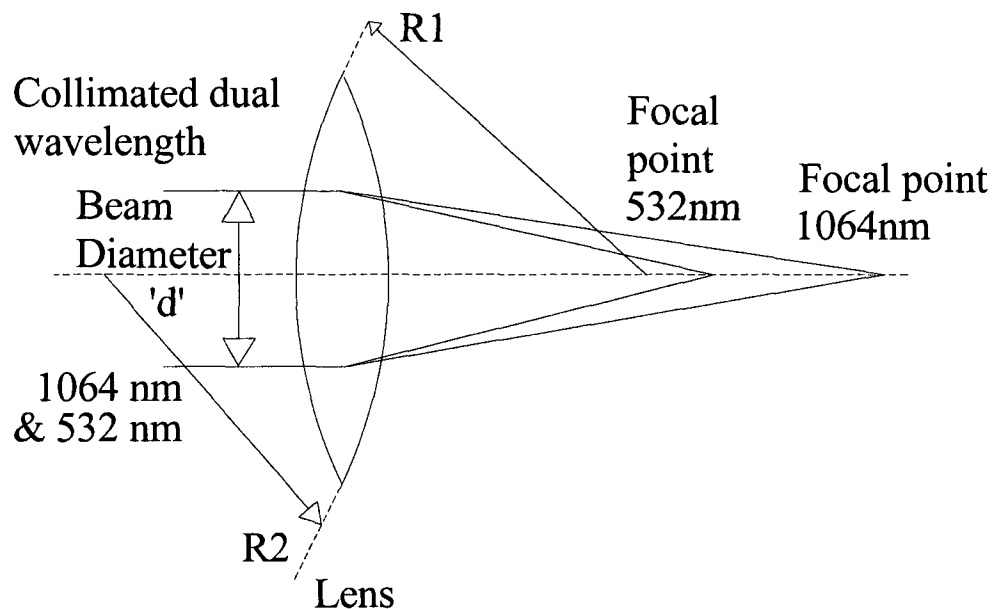
Fig 2.4 *Dual focus chromatic aberration*

Laser beam of different wavelengths refracted at different angles due to different refractive index of the material for different wavelengths. Principle of dual wavelength is explained above with the help of fig.2.4, smaller wavelength focuses ahead of longer wavelength. 'dd' is the distance between the focal points of wavelengths under

30

consideration. The distance 'dd' plays an important role in dual frequency drilling to maintain the continuity. Different laser and optical parameters e.g. radius of curvature of the lens, and beam diameter affects the distance 'dd'. In the next section, modeling has been done to analyze the effect of optical parameters e.g. radius of curvature on dual wavelength drilling.

2.4 Lens design for dual focus drilling

The objective of this work is to drill high aspect ratio hole with dual frequency at minimum possible laser power. To drill with minimum possible power using dual frequency it is important to maintain the continuity between the drilling done by both the wavelengths. In dual frequency micro drilling, smaller wavelength starts machining first as it focuses first, whereas the longer wavelength, which will focus later will just heat the material work piece and also contribute its intensity in drilling at the start. Longer wavelength starts machining from its focal point and drill up to its depth of focus. Hence, to maintain continuity, distance 'dd' should be equal to or lesser then the depth of focus of smaller wavelength or in other words Rayleigh range of longer wavelength should start from or before the point where Rayleigh range of smaller wavelength finishes. On the basis of difference between dd and dofs, drilling can be classified into three categories, as shown in fig. 2.5.

(1) Continuous drilling (dd = dofs)

(2) Overlapped drilling (dd < dofs)

(3) Discontinuous drilling (dd > dofs)
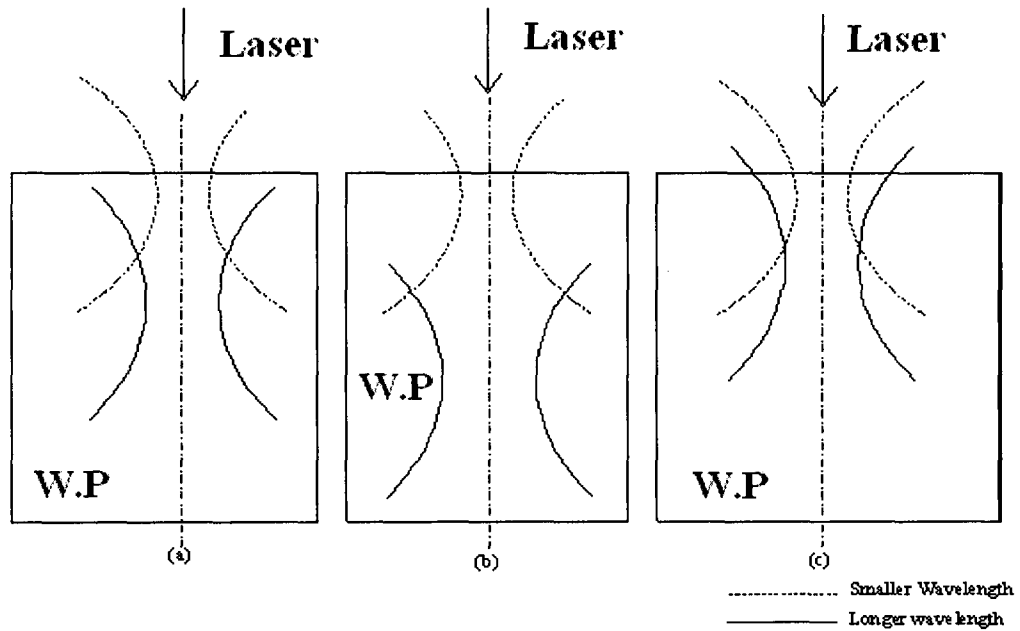
Fig **2.5** *Dual focus drilling (a) Continuous drilling (b) Discontinuous drilling (c)*

Continuous drilling but overlap

Fig 2.5 shows the drilling with dual focus laser beam. In continuous drilling, 'dd' is equal to the depth of focus of smaller, and in case of overlap it is also continuous but depth of focus of longer wavelength overlap with the depth of focus of smaller wavelength which ultimately affects the depth of drilling at a given laser power and will reduce the aspect ratio of the drilled hole. In case of discontinuous drilling 'dd' is higher than the depth of focus of smaller wavelength, longer wavelength takes time to start machining which depends upon power density of longer wavelength, sometimes there might not be any machining from longer wavelength, due to power density is lesser than the damage

32

threshold of the material, as nanosecond pulse laser can only machine at the surface of material. After the depth of focus of smaller wavelength, smaller wavelength starts diverging, due to this energy per unit area reduces, it takes more time to melt the material or to machine the material. To reduce these losses and increase the efficiency, it is important to choose the right radius curvature of lens which is primary parameter in calculating depth of focus and focal point.

2.4.1 Effect of radius of curvature on continuity

Numerical modeling is done to predict the radius of curvature of plano convex lens with respect to different possible wavelength combinations, which satisfies the condition of continuity. The focal length of the particular wavelength will depend on refractive index of the lens material and the radius of curvature of the lens as described in equation (2.3). The distance (dd) between the two foci depends on the difference between the two focal lengths corresponding to two wavelengths as given by equation (2.4).

$$1/fl_\lambda = (N_\lambda - 1) * (1/R_1 - 1/R_2) \qquad (2.3)$$

$$dd = fl_{\lambda 1} - fl_{\lambda 2} \qquad (2.4)$$

where fl_λ & N_λ is focal length & Refractive index of the BK7 lens for a specific wavelength; R_1 and R_2 are the radii of curvature of the two surfaces of the lens. For a plano convex lens, R_2 is infinite, so

$$1/fl_\lambda = (N_\lambda - 1) * (1/R_1) \qquad (2.5)$$

33

and continuity depends upon focal length and depth of focus.

$$\text{Depth of focus (dof)} = 2.44 * \lambda * (fl/d)^2 \qquad (2.6)$$

$$\text{Theoretical spot Size (w)} = 2.44 * \lambda * (fl/d) \qquad (2.7)$$

where fl is focusing length and d is the beam diameter. To study the effect of radius of curvature on continuity, modeling was done by keeping the beam diameter, 'd' constant at 1.6mm for all the wavelength combinations. Fig 2.6 shows the three combinations of wavelengths 1064nm and 532nm, 532nm and 355nm, and 1064 and 355nm, which are higher harmonic order of fundamental wavelength 1064nm.
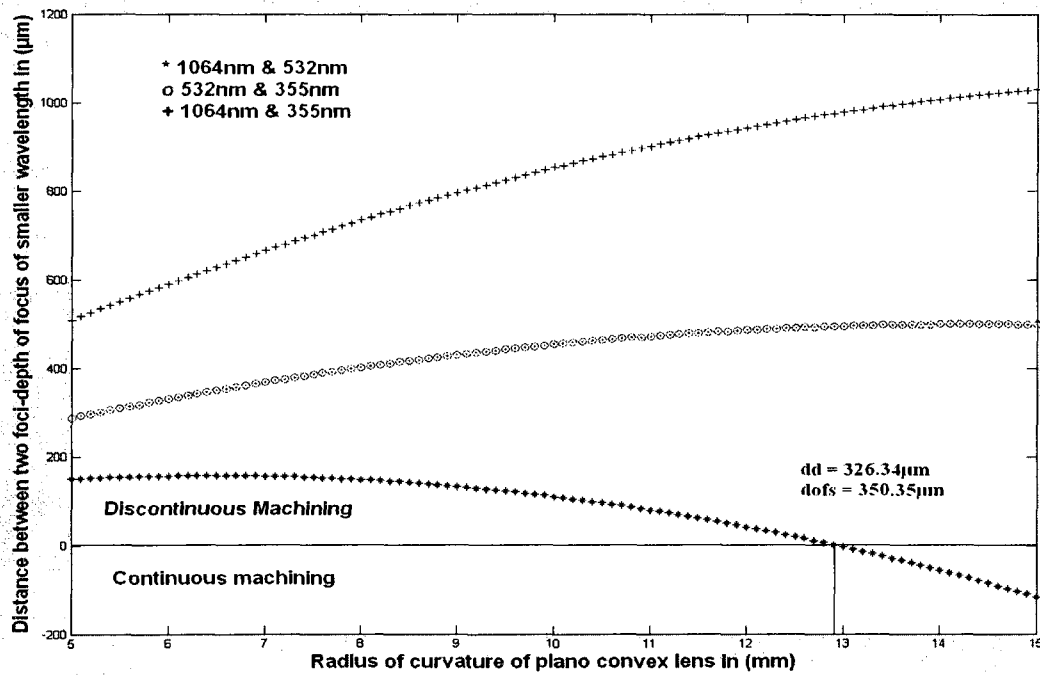
Fig 2.6 *Continuity with respect to combination of wavelengths and radius of curvature of*

lens

34

The difference of dd and dofs with respect to radius of curvature is shown in fig 2.6. In the fig, y-axis shows the difference between distance 'dd' and depth of focus of smaller wavelength, and x-axis shows the radius of curvature of BK7 plano convex lens (R_1). Solid line along the x-axis is where distance 'dd' is equal to the depth of focus of smaller wavelength. Region above the solid line, where dd > dofs, is discontinuous drilling and below the solid line is continuous drilling but with overlap of depth of focus of both the wavelengths. For this work 12.9mm radius of curvature has been selected for 1064nm and 532nm wavelengths because at this radius of curvature, with the mentioned wavelengths the overlapping is minimum therefore drilling can be done with high efficiency in terms of laser energy.

2.5 Intensity distribution of dual focus

For the numerical analysis of dual focus drilling, the Gaussian profile of the laser intensity distribution for TEM_{00} mode is considered to calculate the spot size. Gaussian intensity distribution is given by

$$I = I_0 \exp(-2r^2/w^2) \tag{2.11}$$

Where I is the intensity at any point r along the radius of the beam, w is the beam waist and I_0 is the maximum intensity at the center of the laser beam.
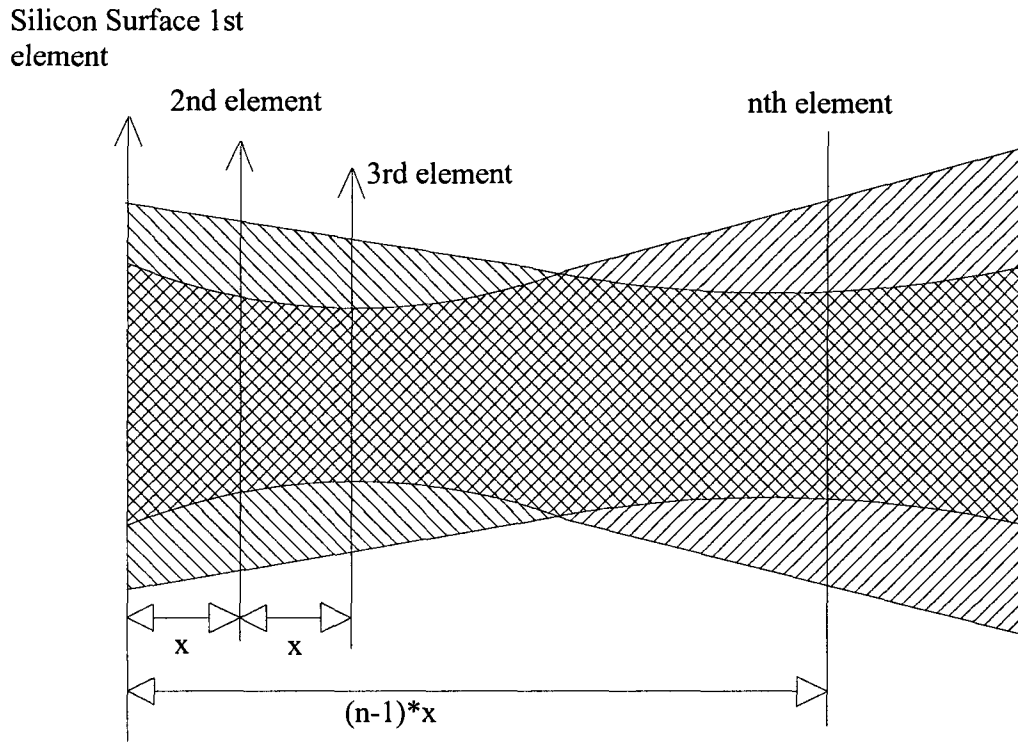
Fig 2.7 *Area considered for calculating the intensity distribution of dual wavelength*

Fig. 2.7 shows the area which is considered to calculate the intensity distribution. Hatching (//) line shows the area of 532nm wavelength and (\\) line shows the 1064nm wavelength and crossed hatching area shows the area under both the wavelengths. For numerical analysis depth of focus is divided into equal elements at the distance 'x' from each other. Fig. 2.7 shows the element at the distance of 'x' from the surface of the silicon wafer which form the 2nd element in analysis as surface of the silicon wafer is 1st element for numerical analysis, and element at distance (n-1)*x from the surface is the nth element in analysis. In this modeling the intensity distribution is calculated at the

36

elements which are separated by 'x' distance along the drilling depth the 'x' is 3 μm. For the numerical analysis the depth was separated into three regions to calculate the intensity distribution on each element. In next section the intensity distribution at the surface of the silicon sample is predicted.

2.5.1 Intensity distribution at the surface of the silicon sample

Initially intensity distribution was calculated at the surface of the sample for each set of wavelengths (532nm and 1064nm) and finally the total intensity distribution was also calculated as shown in Fig 2.8. While calculating the intensity distribution for each wavelength their absorption 35% for 1064nm and 62 % for 532nm on silicon materials [49] was considered. Based on the total intensity distribution, initial spot size of the drilled hole was calculated with respect to damage threshold of silicon. For this part of analysis, efficiency of second harmonic generator was kept at 20% with pulse energy of 600μJ.
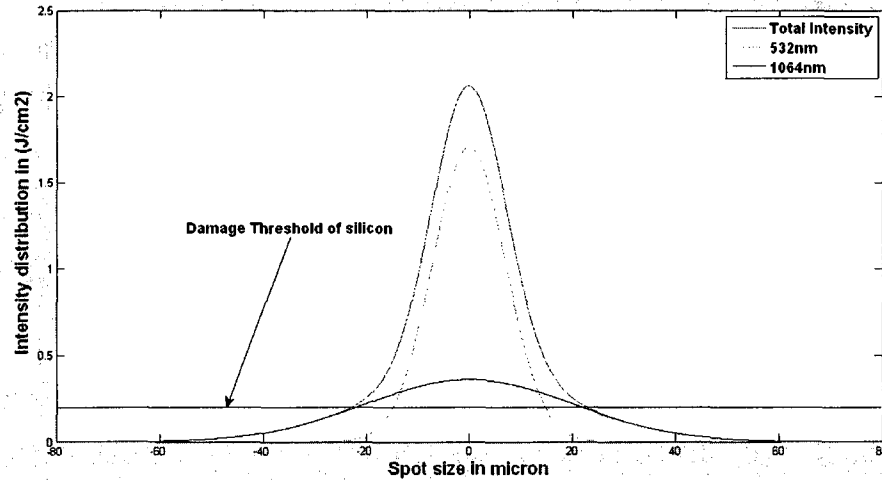
Fig 2.8 *Intensity distribution at the surface of the Silicon sample*

From the intensity distribution curves in Fig 2.8 it can be said that machined spot size (47μm) in dual frequency wavelengths depends on the total intensity distribution shown by the red curve as discussed in section 2.2. Intensity distribution per unit area varies along the depth as the longer wavelength focuses and smaller wavelength spot size varies with Rayleigh range. This effect the total intensity distribution along the depth due to which final drill spot will vary. So to intensity distribution on the elements along the depth in the remaining two regions is discussed below.

2.5.2 Intensity distribution within depth of focus of smaller wavelength

As discussed in the previous section the intensity distribution is similarly calculated on elements within the depth of focus of smaller wavelength. The total intensity distribution

38

was calculated on each element separately. A snap shot of the intensity distribution at three different elements within the dof of smaller wavelength (a) at 50 μm below the surface (b) at 150 μm below surface (c) at 250 μm below the surface is shown in Fig 2.9. From Fig 2.9 it can be seen that the intensity distribution of longer wavelength increases along the depth of focus of smaller wavelength, where as the intensity distribution for shorter wavelength remain almost, due to which the total intensity increases along the depth. Spot size will decreases along the depth, due to the erosion front is propagating into material, laser energy power density reduces due to the increasing distance from the focal plane [66]. Solid line along the x-axis shows the damage threshold value of silicon. Similarly intensity distribution after the depth of focus of smaller wavelength is discussed in next section.
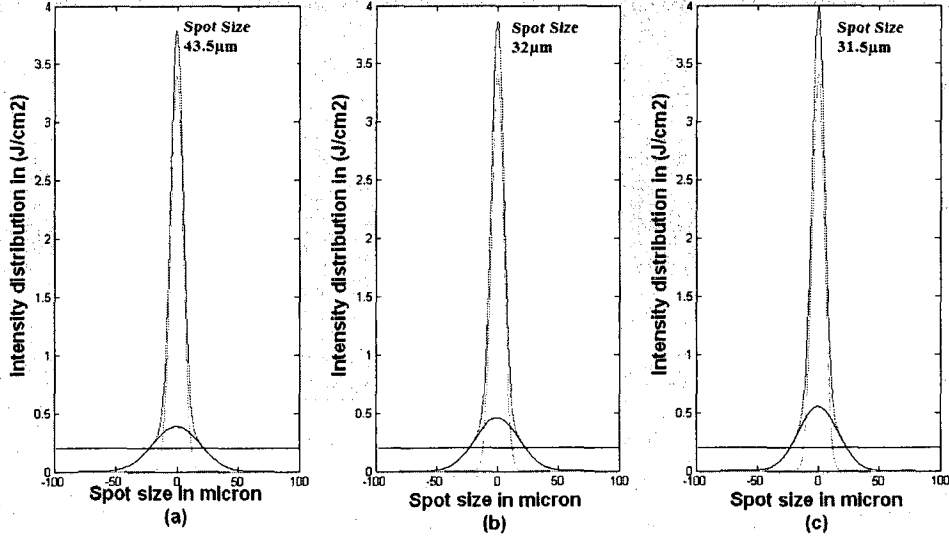
Fig 2.9 *Intensity distribution of 600μJ within depth of focus of smaller wavelength*

2.5.3 Intensity distribution after depth of focus of smaller wavelength

The procedure for calculating the intensity has already been explained in section 2.5.2 and is repeated for the region beneath the depth of focus of smaller wavelength for the whole machining depth. The machining depth is the region where the intensity is more than the threshold fluence of silicon. A snapshot of intensity distribution after the dofs at three different elements at (a) dofs+50μm (b) dofs+150μm (c) dofs+250μm is shown in Fig 2.10.
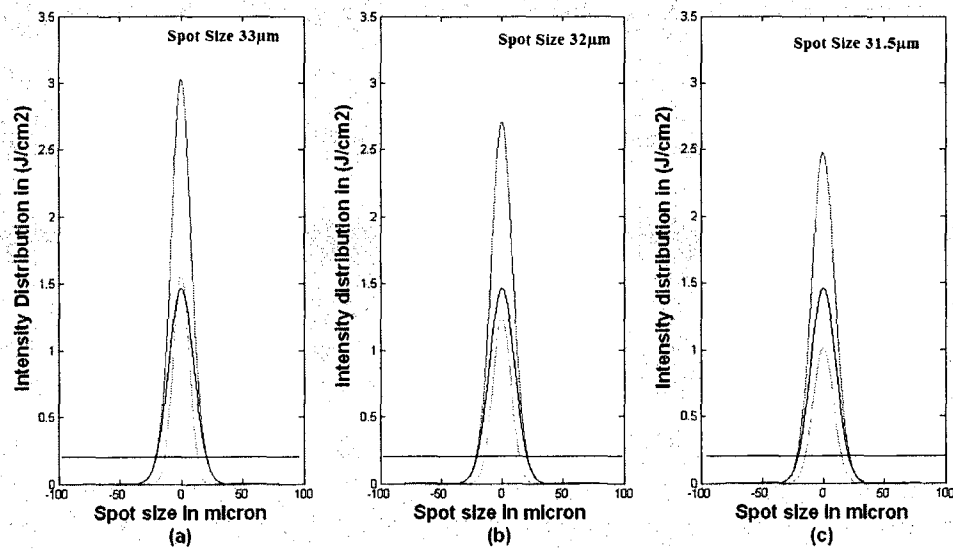
Fig 2.10 *Intensity distribution of 600μJ after depth of focus of smaller wavelength*

From Fig 2.10 it can be said that along the depth of focus of longer wavelength the intensity distribution of smaller wavelength reduces whereas intensity distribution for the longer wavelength remains almost constant, which reduces the total intensity distribution.

Total intensity distribution on each element was calculated and compared with the threshold of the silicon. Machining will take place on the elements where the intensity of the laser beam is above the threshold thus deciding the machining spot size at that element. The calculations were done on all the elements along the depth and final feature shape along the depth was obtained after integrating the spot size at each element, as shown in fig 2.11 values. All further numerical analyses are done on the basis of this discussion. Fig 2.11 shows the predicted profile of the drill hole on the basis of the above discussion. Further study on drilling, the effect of power and efficiency are discussed in the following sections.
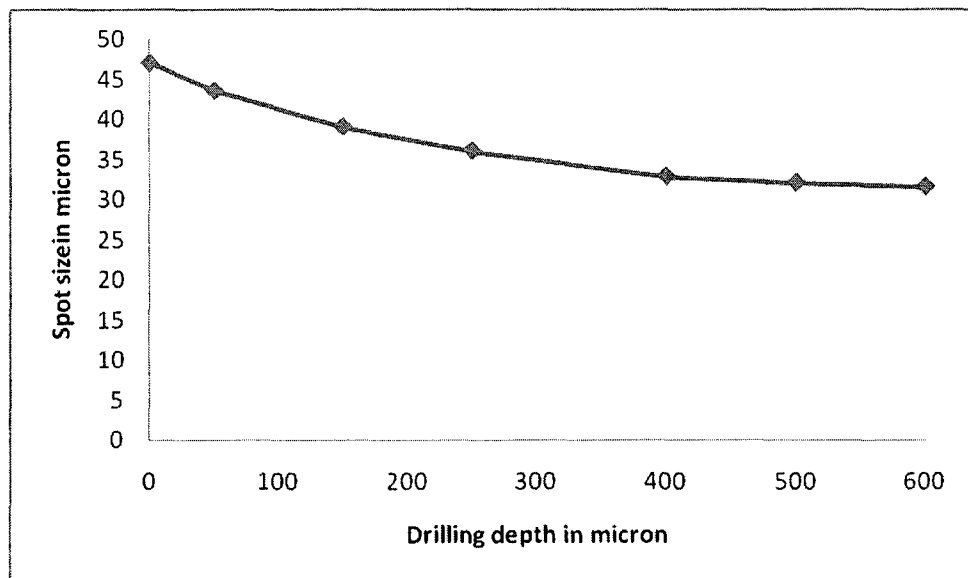
Fig 2.11 *Numerical value of spot size along the depth of drilling with dual wavelength*

2.6 Effect of pulse energy on drilling

Numerical analysis for calculating the spot size was done on the basis of damage threshold of silicon with different pulse energies along the machining depth. Effect of pulse energy on feature size of drilling was analyzed as discussed earlier. Pulse energy of laser can be varied either with average energy of the laser or with repetition rate of the pulse laser. Drilling dimensions were mathematically calculated for different average powers up to possible drilling depths. The variation in the drilling dimensions with average energy is plotted in Fig 2.12
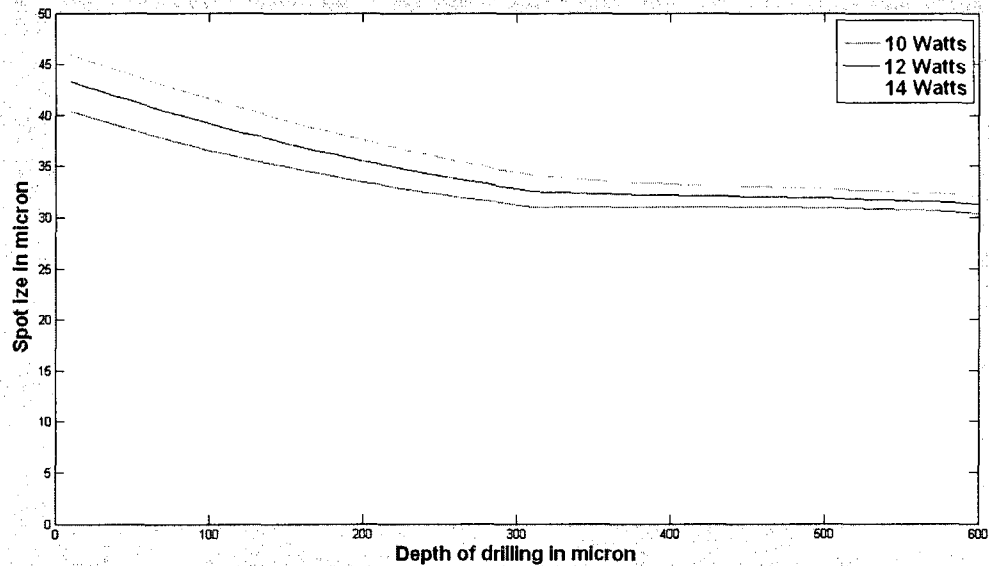
Fig 2.12 *Effect of average power on drilling with 20% efficiency of S.H.G.*

From fig 2.12 it can be said that with the increase in average energy of the laser beam the drilled spot size will increase. The increase in spot size with average energy of the laser is

attributed to changed Gaussian intensity distribution. Since absorption of material depends on wavelength, so power ratio between two wavelengths plays significant role in dual frequency drilling. Efficiency of second harmonic generation varies the power ratio of two wavelengths. So the effect of S.H.G efficiency is discussed, in the next section.

2.7 Effect of second harmonic conversion efficiency on drilling parameters

Energy distribution of wavelengths also play important role on dual frequency laser drilling. In dual frequency laser drilling energy distribution changes the drilling parameters such as depth and spot size of drilling. Each material has its own optical properties with respect to wavelength, like absorption, transmission and reflection. For example silicon absorbs 35% for 1064nm and 62% for 532nm wavelengths respectively [49]. Fig 2.13 shows the intensity distribution of 20 and 50% conversion efficiency of fundamental wavelength.
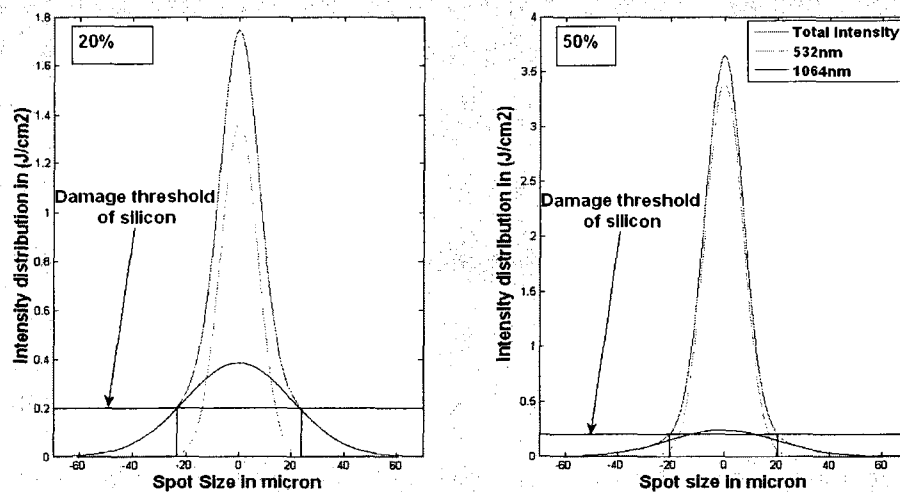
Fig 2.13 *Intensity distribution of 600 μJ with different S.H.G efficiency*

43

Fig 2.13 shows intensity distribution of dual frequency generated from S.H.G crystal having 20 & 50% efficiencies of 600μJ of fundamental wavelength. In fig 2.13 red curve shows the 532nm, blue line shows the 1064nm and green line shows the total intensity distribution of both the wavelength considering absorption for silicon sample at the surface. From fig 2.13 it can be observed that spot size (47μm) at 20% efficiency is high and at 50% efficiency the spot size (34μm) is lesser. It is due to 532nm wavelength having higher absorption as compared to 1064nm and at high efficiency of S.H.G crystal the power of 532nm high, and it is focused at the surface which increases the energy per unit area, hence conversion efficiency of 30% is good for silicon wafer. While 1064nm wavelength is converging at the surface of silicon wafer, due to this energy per unit area is lesser or below the damage threshold of silicon, due which the spot size reduces. From this calculation it shows that S.H.G efficiency play significant role on feature size of dual focus microdrilling.

Theoretical maximum efficiency of KTP crystal is 30%. Numerical analysis was done with three different efficiencies of harmonic generation possible with KTP crystals with nano second lasers and 50% conversion efficiency of other S.H.G crystal as discussed in earlier section. Variation in spot size along the depth of drilling was plotted in Fig 2.14.
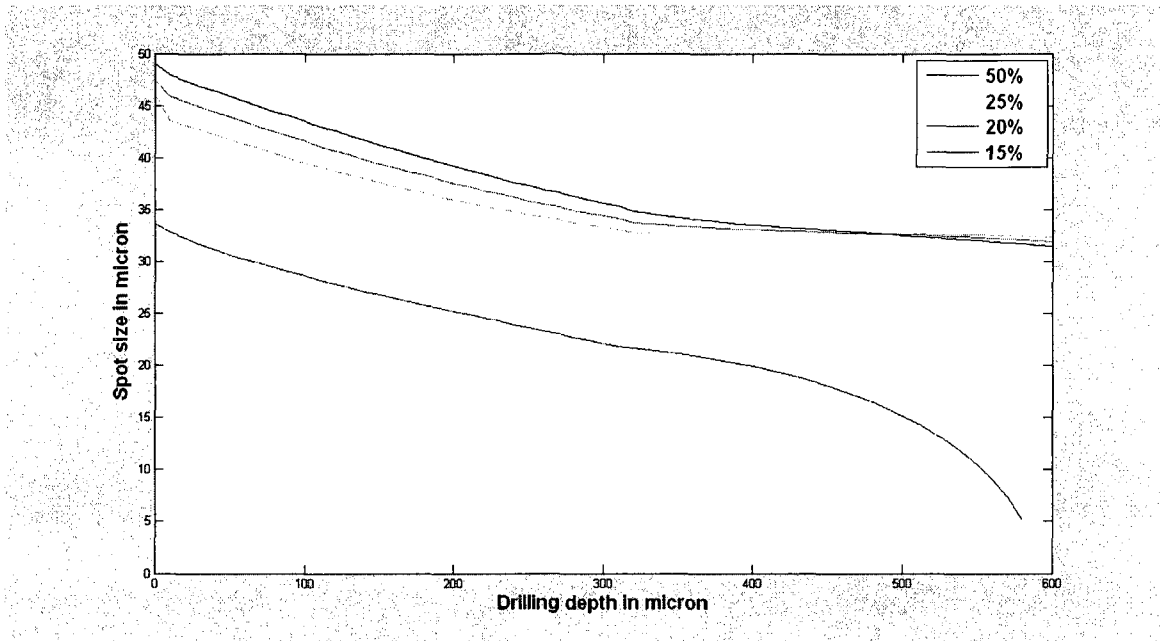
Fig 2.14 *Effect of Second Harmonic generation Efficiency at 600μJ.*

From Fig 2.14 it can be seen that with the increase in the efficiency of second harmonic generation the spot size reduces at beginning, whereas with low efficiency of generation the variation in spot size along the depth of drilling is quit high as comparison to higher efficiency generation. With increase in efficiency of second harmonic generation kerf angle will be reduced. Kerf angle is defined as the angle generated from the difference in widths between the top and bottom of the drilled hole. However for silicon, when the conversion efficiency of 50% the 1064nm wavelength will not have enough power to drill if 532nm wavelength is diverging. Fig 2.15 shows the comparison of single and dual wavelength drilling with same power.

45
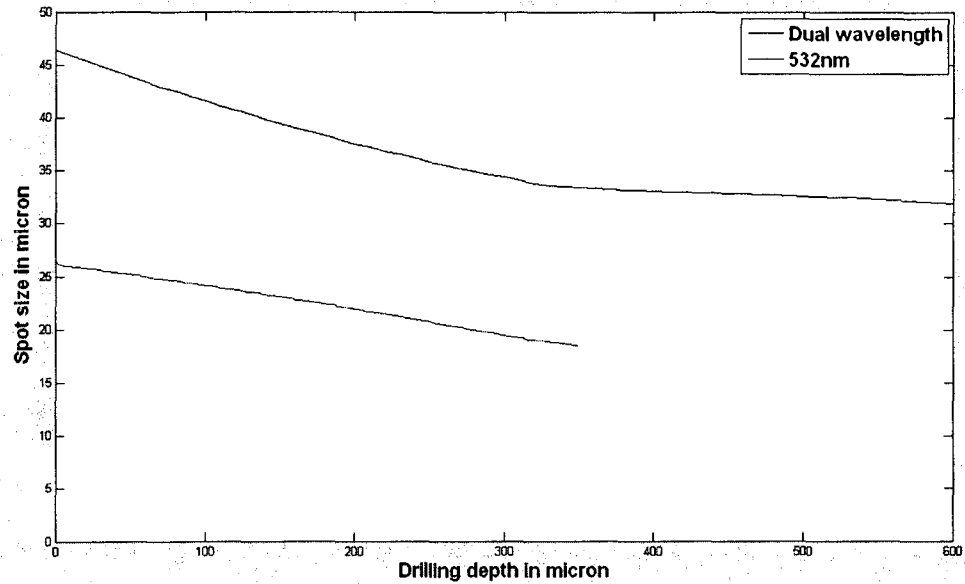
Fig 2.15 *Drilling with single and dual wavelength at same power*

Fig 2.15 shows the drilling with single wavelength of 532nm and dual wavelength of 532nm and 1064nm with laser pulse power of 600μJ and for dual wavelength S.H.G crystal having efficiency of 20%. From the fig it is shown that at same laser power drilling depth is less when compared with dual wavelength as it is focuses at two different points which provides optimal intensity distribution to increase the aspect ratio. In single wavelength most of the energy is lost in conduction to surrounding as energy density is high in single wavelength, which increase the heat affect zone and the spot size.

2.8 Summary

From the theoretical modeling it can be summarized that dual wavelength drilling can act as a tool for high aspect ratio drilling, due two both wavelength focused at two foci which increases the depth of drilling. Different laser parameters have been studied and the effect of those parameters on drilling has been predicted. From the results of the modeling it can be concluded that diameter of the drilled hole can be controlled with the help of laser power whereas depth of drilling can be controlled with all the three laser parameters laser power, rep. rate and number of pulses hitting the surface. Modeling has been done to predict the effect of simple harmonic generation efficiency of the drilling parameters. Effect of dual wavelength intensity distribution has been studied in detail with MATLAB and it can be predicted from the modeling that kerf angle of the drilled holes can be decreased with dual wavelength drilling which is not possible with single wavelength.

Chapter 3 Experimental setup

3.1 Introduction

As discussed in the Section 1.8 of this thesis objective of this research work is to perform, high aspect ratio drilling with a dual frequency nanosecond laser on silicon wafer. To accomplish this task a simple optical setup with minimum alignment requirements has been designed. The experimental setup consists of two parts, first part was designed in such a way that the primary frequency from the nanosecond laser source was converted into dual frequency and the second part of the design consists of optimizing the setup for micro drilling. In the first part, the frequency doubling was achieved by second harmonic generator crystal. The output of S.H.G was two beams on the same axis, one having the primary frequency of the laser and the second which was frequency doubled. As such the output beams have the fundamental wavelength of 1064nm and the frequency doubled wavelength of 532nm. The challenge was to achieve maximum efficiency by proper procedure for alignment.

The second part of the experimental setup was to use dual wavelength to focus at different points along the optical axes to achieved high aspect ratio microdrilling. The distance between the focal points can be varied by the beam diameter, radius of curvature of the Plano convex focusing lens and the lens material, as discussed in chapter 2. The

challenge in this part is to select the optimum distance for achieving continuity in drilling thick material at minimum power.

3.2 Optical setup description

The optical setup has been designed in such a way that maximum conversion efficiency can be achieved with minimum reflection losses of the fundamental wavelengths and micro drilling can be achieved with minimum alignment by using both second harmonic and fundamental wavelengths simultaneously. Schematic of the experimental setup which comprises of two parts is shown in fig 3.1.
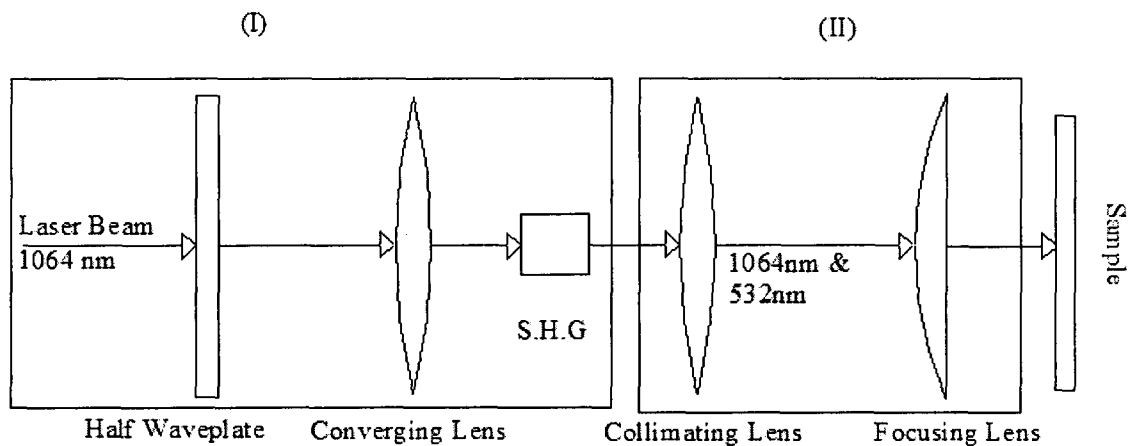
Fig 3.1 *Sketch of experimental setup*

In this work a nanosecond laser with fundamental wavelength of 1064 nm is used for experiments. The first part of the alignment is aimed to achieve the maximum efficiency from the second harmonic generator. Using polarization and focusing optics before the

S.H.G crystal. Half wave plate was used to change the polarization of fundamental wavelength after which a converging lens was used to change the energy density of the beam impinging on the second harmonic generator. The S.H.G crystal was mounted with maximum degree of freedom on all the three (x, y, and z) axes to achieve the maximum alignment flexibility.

Output of the S.H.G crystal is a diverging laser beam with dual frequency. The divergent laser beam was collimated to achieve a desired constant diameter using a convex lens. Collimated beam was then focused on to workpiece for high aspect ratio microdrilling. The functionality, selection, and the alignment of the major components in the experimental setup are discussed in the subsequent sections.

3.3 Maximizing the conversion efficiency of S.H.G.

As shown in fig 3.1, the first part of experimental setup comprises of nanosecond laser, waveplate, converging lens and S.H.G crystal for dual frequency generation. The selection of the components and the alignment requirement with respect to maximum conversion efficiency is discussed below.

3.3.1 Nd: YVO4 Laser (Neodymium Doped Yttrium Orthvanadate)

Laser used for the experimental work was manufactured by Coherent laser (model PRISMA 1064-16V). This is a solid state laser with Nd: YVO_4 (Neodymium doped

Yttrium Orthvanadate) crystal that has an average power of 14W. Among the various available laser crystals like Nd: YAG, Nd: YVO$_4$ and Nd: YLF for diode laser pumping, Nd: YVO$_4$ laser has the advantage over the others due to temperature control of a diode laser, lower dependency on pump wavelength, high absorption coefficient and high damage threshold [50].

This laser has a dual output; continuous and pulsed, with tunable repetition rates ranging from 20-100 kHz and output power tunable through the diode current (13 – 34 Amps). Repetition rate is number of pulses coming out from the laser in one second. By varying diode current average power of the laser will be increased due to increase in excitement of atoms in the crystal at constant repetition rate, which increases peak pulse power resulting in material removal.

3.3.2 Second Harmonic Generation

Lasers generate coherent radiation at many wavelengths ranging from meter wavelength region to the soft X-rays region. However it is not possible to produce light covering all wavelengths of interest in spite of the fact that a large number of active materials are available and lasers can be built using them. Therefore it is necessary to transform the frequency of light generated by the laser into light of desired frequency. Harmonic generation, sum and difference frequency generation and parametric oscillation are some

common processes that utilize the principle of nonlinear optics for laser light frequency transformations.

Lasers produce light of the field strength of the order of 10^7 to 10^{11} V/m, which are of the order of the atomic field strengths. Therefore, the intense light of the lasers is in a position to cause non linearity of P and influence the optical parameters of the medium as shown in Fig.3.2. When the electric field E in the light is very large, the parameters χ, and ε become the functions of E. ε_0 is the permittivity of free space and χ is dimensionless constant known as electric susceptibility of the medium. Since the directions of P and E coincide in an isotropic medium, we can express χ as power series in the field strength as,
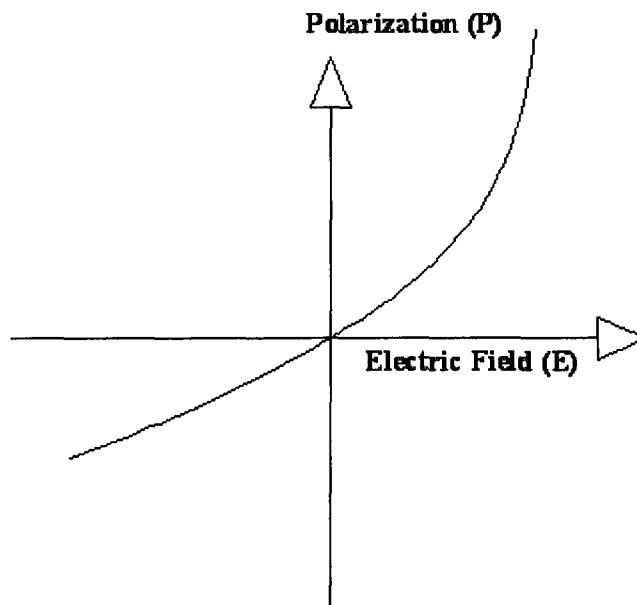
Fig 3.2 *Non linear medium [51]*

52

$$\chi(E) = \chi_1 + \chi_2 E + \chi_3 E^2 + \ldots\ldots\ldots\ldots \tag{3.1}$$

$$P = \varepsilon_0 \, \chi(E) \, E \tag{3.2}$$

$$P = \varepsilon_0 \, (\chi_1 E + \chi_2 E^2 + \chi_3 E^3 + \ldots\ldots) \tag{3.3}$$

Where χ_1 is linear susceptibility and is much greater than the coefficients of the non linear terms χ_2, χ_3 and so on. Non linear terms contribute only at very high amplitudes of electric fields. The second order nonlinear polarization is given by equation (3.4)

$$P_2 = \varepsilon_0 \, \chi_2 E^2 \tag{3.4}$$

And third order nonlinear polarization by equation (3.5)

$$P_3 = \varepsilon_0 \, \chi_3 E^3 \tag{3.5}$$

Non linear polarization leads to nonlinear optical effects. Materials, in which polarization exhibits non linear dependence on the field strengths, are called non linear media. In optically isotropic materials, the coefficients of even power of E in equation (3.3) are zero. But in case of anisotropic materials, coefficients of both odd and even powers of E exist. Strictly speaking, any medium becomes non linear provided the electric field of the incident radiation is very high.

Second harmonic generation which utilizes the nonlinearity was first demonstrated by P. A. Franken, et.al, at the University of Michigan, in 1961. The demonstration was made

possible by the invention of the laser, which created the required high intensity

monochromatic light [52]. In S.H.G, photons interacting with a nonlinear material are

effectively combined to form new photons with twice the energy and therefore twice the

frequency and half the wavelength of the initial photons [53].
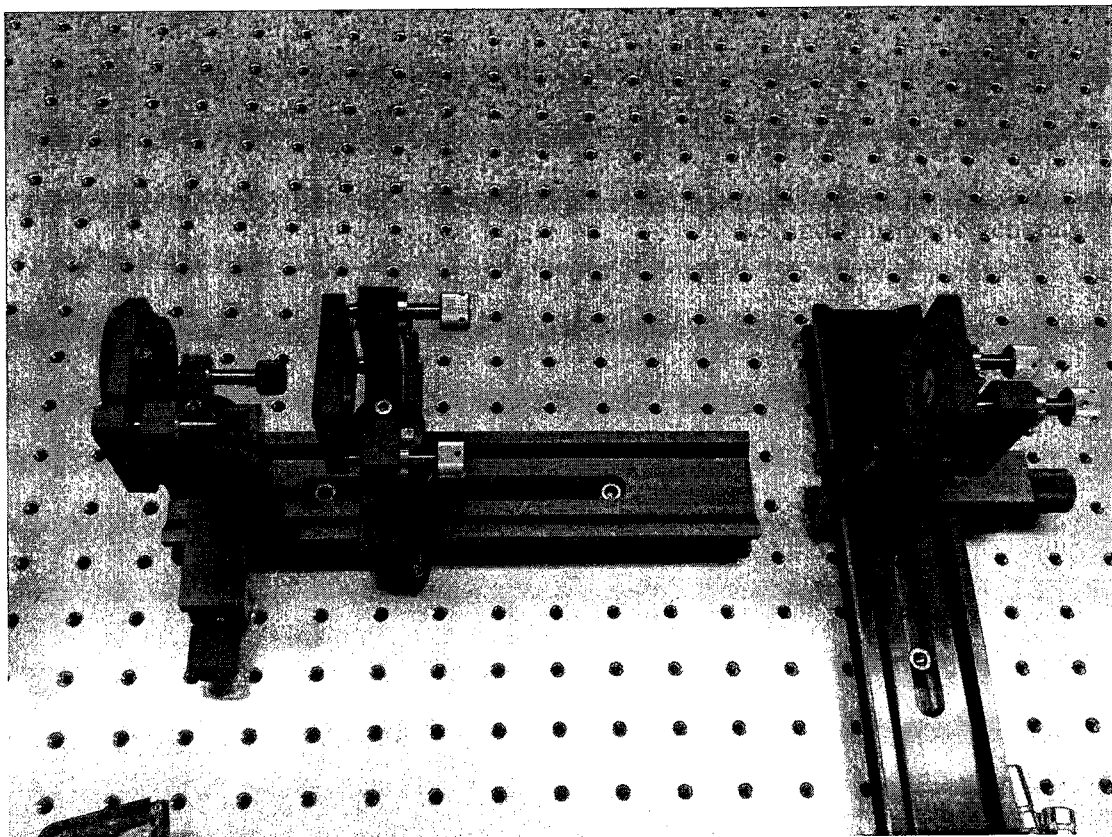
Fig 3.3 *S.H.G experimental setup*

Fig 3.3 shows the optical setup for second harmonic generation where the 1064nm

wavelength from the laser source, after passing through the waveplate and converging

lens, impinges on the nonlinear crystal to generate dual frequency light comprising both

1064nm and 532nm wavelengths. Most commonly used materials for second harmonic

generation are Lithium Triborate LiB_3O_5 (LBO), beta-BaB_2O_4 (BBO) and Potassium Titanyl Phosphate $KTiOPO_4$ (KTP). These commonly used crystals are either negative crystal or positive crystals. In a negative crystal, if the fundamental light is a linearly polarized ordinary wave, the resulting second harmonic will be an extraordinary wave. The reverse is the situation in case of positive crystals [54]. In this work, for all the experiments KTP crystal is used as Second harmonic generator, which is described below.

3.3.3 Potassium Titanyl Phosphate KTiOPO4 (KTP)

KTP is a widely used material for frequency-doubling Nd: YAG and other Nd-doped laser systems that emit 1064nm fundamental wavelength [55]. KTP has some properties that make it unique for second-order nonlinear-optical applications and S.H.G of Nd lasers in particular. Its large nonlinear coefficient combined with low absorption and wide acceptance angle [56 - 58], makes it the preferred doubling crystal, when the available peak power is limited. The unusually large temperature bandwidth of KTP is particularly advantageous for maintaining pulsed energy stability of the frequency converted beam [58]. The temperature bandwidth and relatively good thermal properties provide advantage to KTP for frequency doubling of lasers with high average powers [59]. Experiments of intracavity frequency doubling have shown that KTP is much less susceptible to bulk damage than, other crystals at relatively high average-power levels [60, 61]. Moreover, KTP has very low absorption loss at 1 μm wavelength, makes this material the primary choice of all interactivity frequency doubling applications for

nanosecond lasers at 1064nm wavelength. Some of the properties of KTP crystal are listed in table 3.1.

Properties	Values
Crystal structure	Orthorhombic, Space group Pna2, point group mm2
Cell parameters	a = 0.6404 nm, b = 1.06nm, c = 1.28 nm, Z = 8
Melting point	1172°C
Curie point	936° C
Mohs hardness	≈ 5
Density	3.01 g/cm^3
Colour	Colourless
Hydroscopic susceptibility	No
Specific heat	0.1643 cal/g°C
Thermal conductivity	0.13W/cm/°K
Electrical conductivity	$3.5 * 10^{-8}$ s/cm(22°C,1 kHz)

Table 3.1 *Properties of KTP crystal [62]*

3.3.4 Alignment for second harmonic generation.

In dual frequency laser micromachining, conversion efficiency of SHG is an important aspect. Change in efficiency will change the drilling profile due to change in the ratio of fundamental wavelength and second harmonic wavelength. Efficiency of the S.H.G

56

depends on alignment axes of crystal with respect to polarization of laser beam and position of the crystal with respect to the axis of the laser beam. Efficiency of the S.H.G is given by equation (3.6) [63]

$$\eta = P_{2\omega}/ P\omega = L^2 k \ (P\omega * \sin^2 (\Delta k * L/2))/ (A \ (\Delta k * L/2)^2 \qquad (3.6)$$

Where $P_{2\omega}$ is power of second order wavelength, $P\omega$ is the power of fundamental wavelength, L is the length of the non-linear crystal, k is a constant relative to the fundamental beam and the crystal material, A is the area of the fundamental beam on the crystal surface, and Δk is the wave number difference. The conversion efficiency depends on the length of the crystal (L), the power density which is a function of A, and the phase mismatch (Δk) [63]. The harmonic energy is at maximum when $\Delta k = 0$, which is termed phase matching. It is possible by the choice of polarization and direction of propagation it is often possible to obtain $\Delta k = 0$. The non-linear crystal is machined to make the plane of beam incidence perpendicular to the optical axis.

In order to get maximum efficiency in terms of wavelength energy, the orientation of the crystal should be phase matched. This can be done by phase matching the angle by which the crystal is rotated along the optical axis. In this kind of phase matching, SHG crystal rotated along x-axis, to form a 45° angle between the diagonal of the polished surface and the direction of polarizing of the input light. This can be achieved by rotating the crystal

along the x-axes or rotating the polarization with the help of half waveplate as shown in fig 3.9.
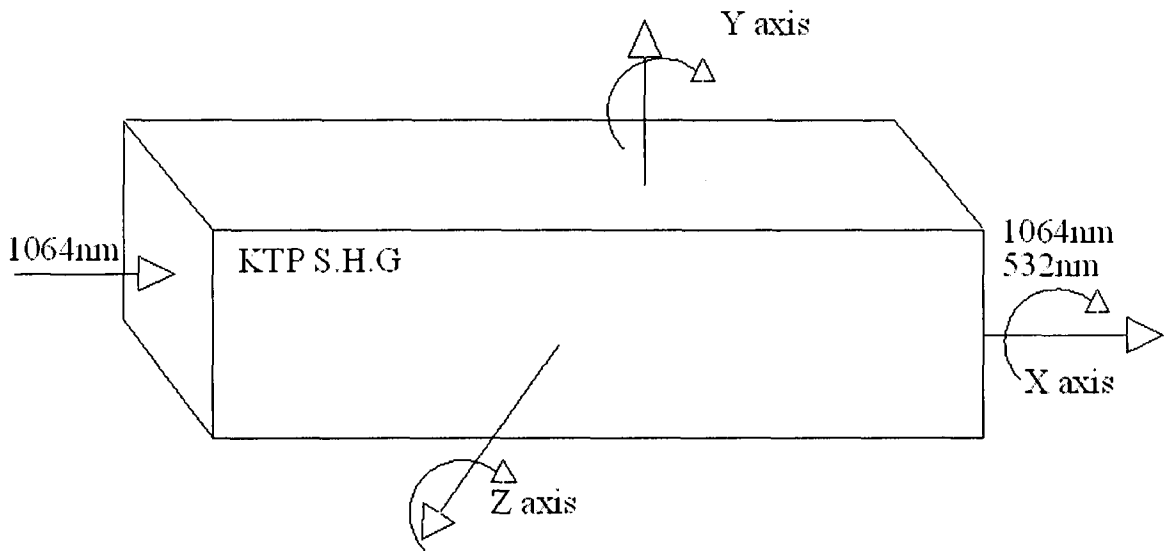
Fig 3.4 *Alignment of SHG crystal*

All the adjustments related to SHG or focusing optics were done at lower power levels for avoiding the risk of optics damage. The specific alignment requirements with respect to crystal axes are shown in fig 3.4. In order to phase match the crystal with polarization of the incoming beam, half waveplate was rotated along the x-axis. To get the incoming beam to incident perpendicular to the polished face of the crystal, the crystal was rotated the y and z axis. Converging lens was used to change the area of the beam impinging on the crystal. Considering the damage threshold, the crystal was placed at short distance away from the focal point of the converging lens. Every step in the alignment plays role

in increasing the efficiency, the power of the second harmonic light was measured and optimized after every step. Since the output has two wavelengths, and the requirement to measure the power of one of the wavelengths following scheme was devised as show in fig 3.5.
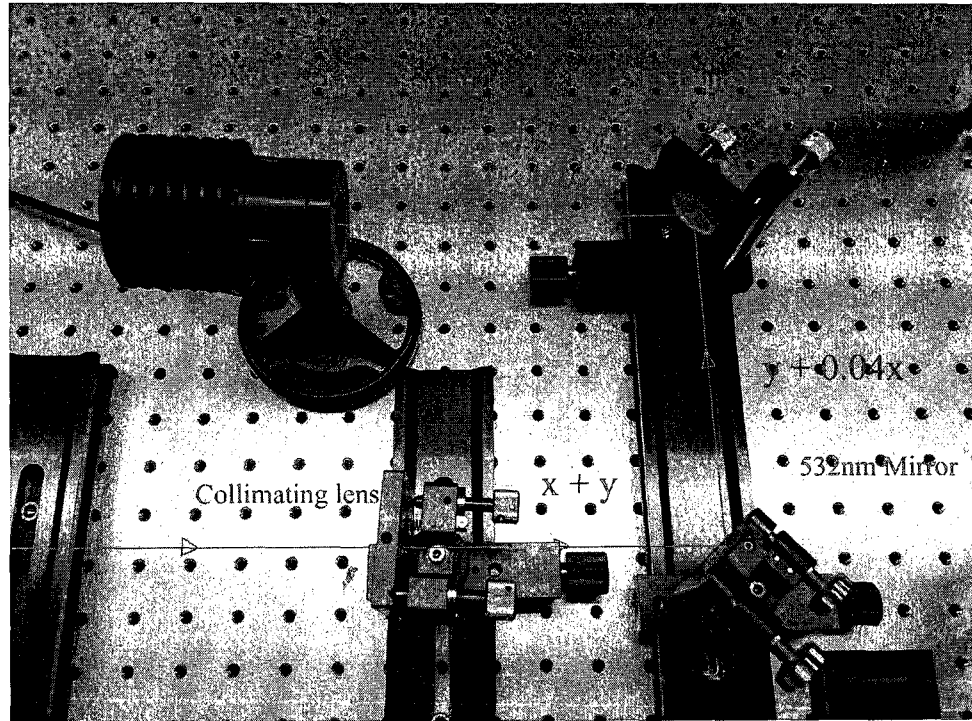
Fig 3.5 *Experimental set up for measuring the conversion efficiency of SHG.*

Power is measured (power meter LabMax-TOP) after reflecting the beams using two mirrors having 100% reflection of 532nm and 4% for 1064nm wavelengths. Output power measured after the crystal comprises the power of both 1064 and 532nm represented by x and y respectively in the fig. subsequent reflections reduces the x component while maintaining the y component, from which the individual powers of

1064, and 532nm and the conversion efficiency of S.H.G crystal can be determined. All these adjustments were iteratively done to maximized the S.H.G efficiency

Diode Current Ampere	Average power (W) after first mirror (y +0.04x)	Average power (W) after second mirror (y +0.0016x)
25	1.575	1.5
26	1.78	1.67
28	2.03	1.91
30	2.23	2.12
32	2.5	2.38
34	2.63	2.5

Table 3.2 *average power of 532nm wavelength after reflecting mirror*

Table 3.2 shows the average power 532nm wavelength after reflecting from mirror as discussed above.

3.4 Optical setup for micro drilling

Optical parameters were optimized to obtain good machining results and also to avoid risk of accidents. In laser beam alignment it is important to impinge the laser at the centre of the optics to get the maximum transmission and to reduce the reflectivity from the

60

optics. It even more important in case of laser drilling not only to reduce the losses but also to reduce the chances of accident due to scattering and reflection. In this part of the experimental setup, the dual frequency divergent beam was collimated with the help of a convex lens. By this collimating lens beam diameter can also be modified as given below

$$d_1 / FL_1 = d_0 / FL_0 \qquad\qquad (3.7)$$

Where d_0 and d_1 is initial and collimated diameter of the beam, FL_0 and FL_1 is focal length of the converging and collimating lens. Combination of collimating lens and plano convex focusing lens can affect the beam diameter, focal spot size, depth of focus and distance between two foci which are very important in optimization of high aspect ratio micro drilling.

3.4.1 Plano convex lens

A lens is an optical device with axial symmetry which transmits and refracts light, or can converge or diverge a beam. A plano-convex lens mainly known as a convergent or positive is a lens consist of one flat side and variable thickness, the lens thickness is more in the centre as compared to the edges as shown in Fig. 3.6 [64].
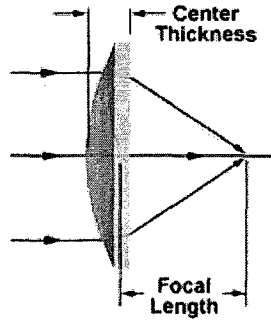
Fig 3.6 *Plano convex lens [65]*

Considering the principle of optics, the focal length of the plano convex lens is given by

$$1/FL_\lambda = (N_\lambda-1) * (1/R_1)$$ (3.8)

Where FL_λ & N_λ is focal length & refractive index of the lens for a specific wavelength; R_1 and R_2 are the radii of curvature of the two surfaces of the lens, R_2 is infinite for Plano convex lens. In the experiments, a collimated light with beam diameter of 1.6mm was made to impinge on a BK7 plano convex lens (R_1 = 12.9mm). 1064nm and 532nm wavelength focused at two different foci and as discussed in theory for micro drilling.

3.5 Summary

The setup was designed and aligned for drilling with dual as well as single wavelength using a simple setup. Dual wavelengths were generated with KTP nonlinear crystal, aligned for maximum efficiency with respect to conversion of fundamental wavelength to second harmonic. The dual wavelength light was focused on the substrate with a common

focusing lens. Parameters like radius of curvature of the focusing lens, and the beam diameter were maintained constant as discussed in chapter two for continuous drilling with minimum available power.

Chapter 4 Experimental results and discussion

4.1 Introduction

Experiments for dual wavelength and single wavelength pulsed laser drilling were done by configuring the setup discussed in the previous chapter. Effect of nanosecond pulsed laser on drilling of silicon wafer was studied with respect to different laser and optical parameters. The set of experiments was designed to evaluate material removal rate with respect to laser power, both in single and dual wavelengths and optimize the parameters to achieve continuity using dual wavelength at minimum power. Experiments were performed in ambient condition with different repetition rates, laser energies and with different number of pulses that contributes towards drilling. In all the cases the drilled holes were studied with the help of SEM images.

4.2 Influence of laser energy

Laser energy is the primary parameter in laser drilling which affects the spot size, depth of machining, and kerf angle. To study the impact of laser energy on the silicon wafer, experiments were done at different laser energy levels with all other parameters maintained constant. Repetition rate was maintained at 20 kHz; radius of curvature of plano convex lens R_1 12.9 mm, the collimated beam diameter of 1.6 mm for single as well as for dual wavelength drilling.

All materials transmit, reflect, or absorb light at different ratios depending on their optical properties. The light absorbed by the material is converted into heat and will contribute in drilling. Absorption of light within a material depends upon the wavelength of light. Material, like silicon has different optical absorption at different wavelengths, as mentioned earlier. For all energies, different spots were drilled with 1064nm, 532nm and dual wavelengths. The spots were studied with SEM images and discussed in the subsequent sections.

4.2.1 Influence of laser energy on drilling with 1064nm wavelength

As discussed above, to study the effect of energy a wavelength of 1064nm, silicon wafer was drilled with different energies ranging from 150μJ to 600μJ sample SEM images spots drilled on silicon wafer using 1064nm at different powers are shown in Fig. 4.1

(a)

(b)

66
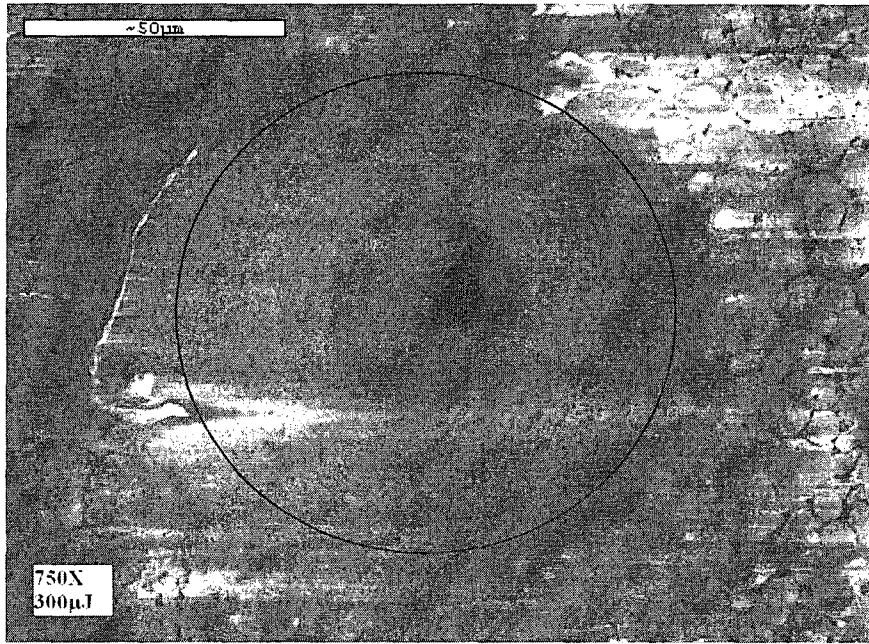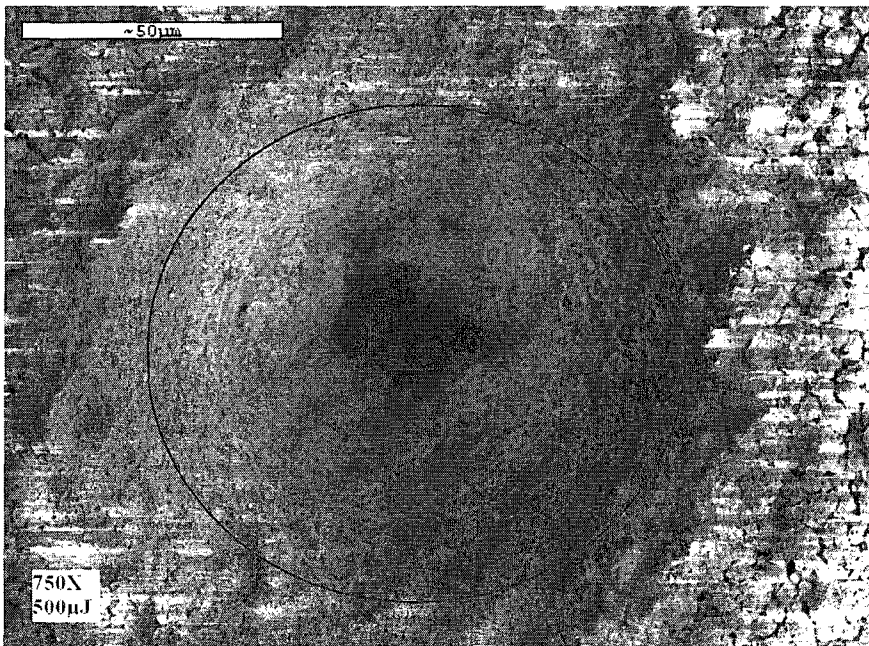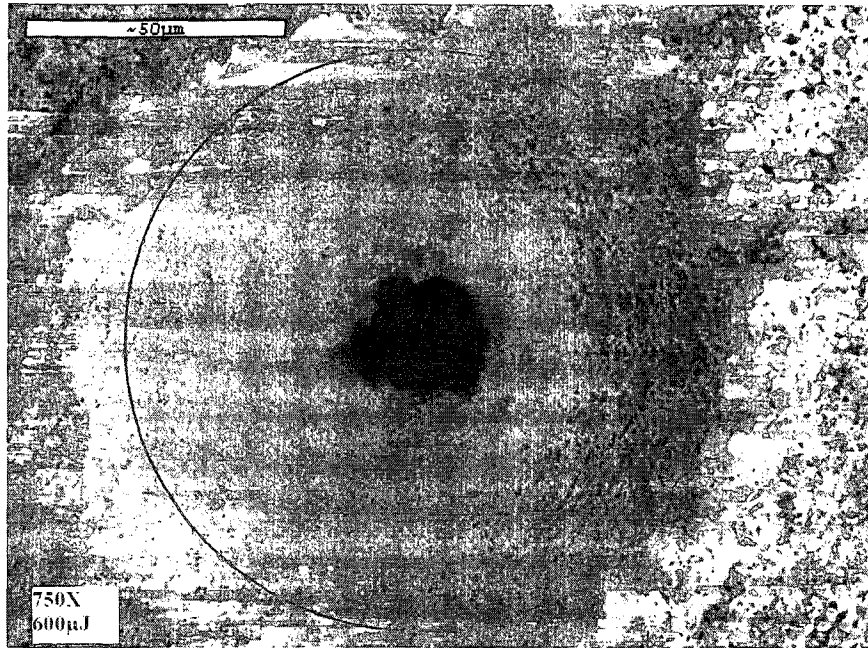
(c)

Fig 4.1 SEM images of different spots drilled with 1064 nm for 3 second

From the Fig 4.1 it can be observed that with increase in the laser pulse energy drilled

spot size on silicon wafer also increases. Increase in laser pulse energy also increases the

depth of drilling and reduces kerf angle. Kerf angle is defined as the angle generated from

the difference in widths between the top (ϕI) and bottom (ϕB) surface of the drilled hole

as shown in fig 4.2. As it seen from S.E.M image (ϕB) increases with increase in the

pulse energy which results in lesser kerf angle. Top diameter (ϕI) also increases with

increase in the pulse energy.

Kerf angle

ØI Top Surface

Work Piece Thickness

ØO Bottom Suface
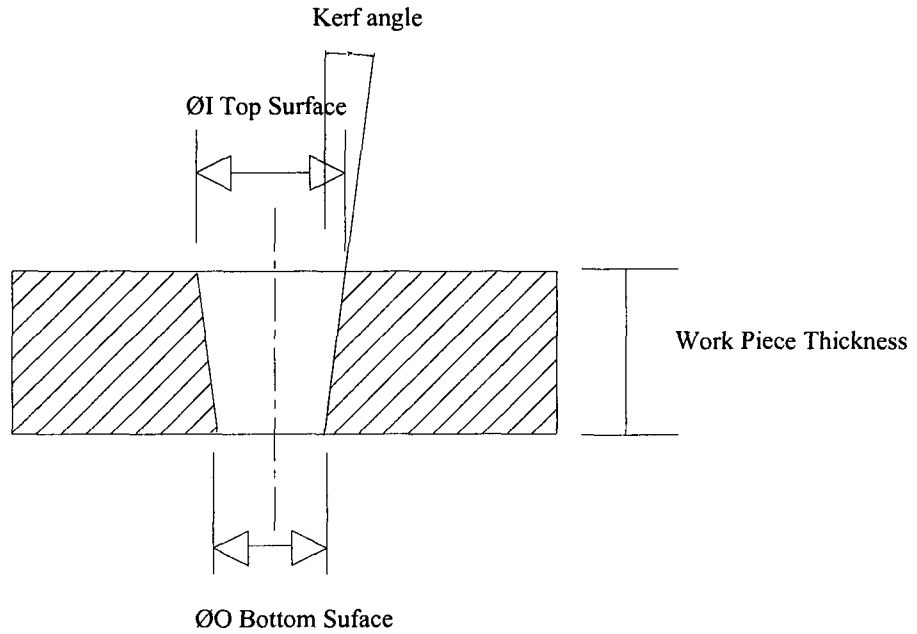
Fig **4.2** *Kerf angle diagram*

Laser pulse energy of the beam can also be changed by varying the repetition rate. Repetition rate is important parameter of the pulsed laser drilling. In this section of experiments nanosecond laser was used that can be tunable for different repetition rates starting from 20 kHz to 100 kHz. Different spots were drilled at different repetition rates thus each time vary the number of pulses hitting the silicon wafer sample consequently varying pulse energy. Theoretical modeling was already done with respect to equation 4.1 given as

Energy per pulse (Joules) =Energy average (watt)/repetition Rate (kHz).   (4.1)
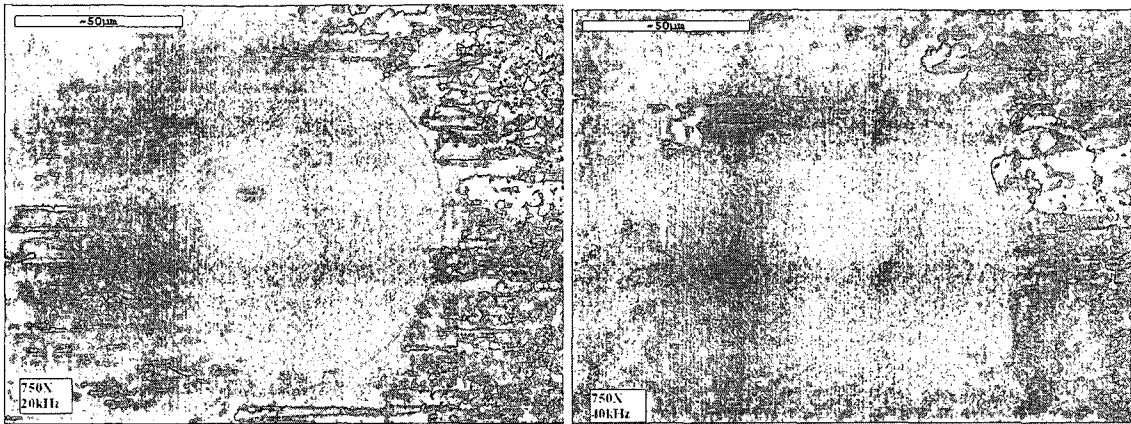
(a) (b)
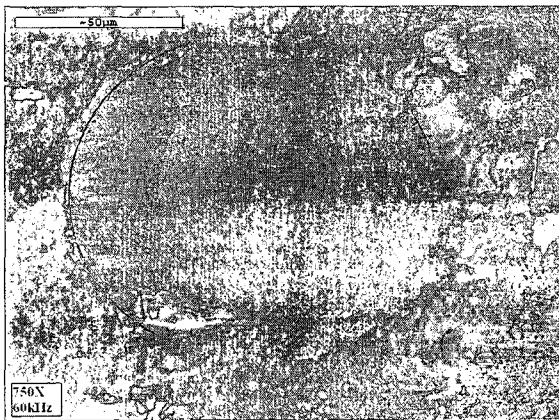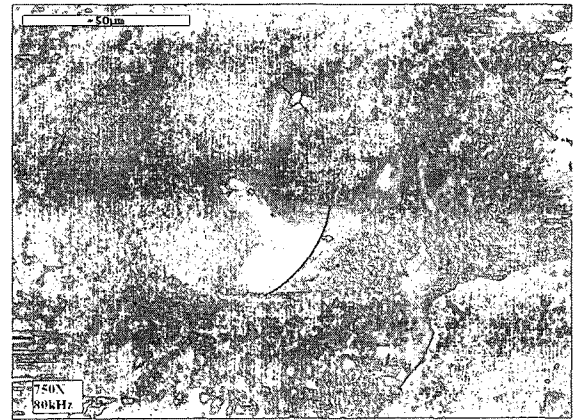
(c) (d)

Fig 4.3 *SEM image at 750X of different spots drilled with same energy for 3 second at different repetition rate*

Experiments were done with different rep. rate values at approximately same average laser power for same time of machining and obtained results are shown in Fig 4.3. From SEM image it can be concluded that drilling at 20 kHz is deeper and wider as compared to the drilling in fig (c) and (d). Fig 4.3 (c) shows shallow depth of drilling when compare

with fig (b). Fig 4.3 (d) Shows material condenses in hole due to lack of sufficient energy which is require to eject the molten material from the hole. From this set of experiments it can be concluded that drilling spot size decreases at higher repetition rate. This decrease in drilled spot was due to the decrease in the peak energy with the increase in repetition rate according to equation 4.1. Effect of lens focal length on spot size was discussed in next section.

The damage threshold value of material affects the amount of energy that it requires for ablation. However since the damage threshold in nanosecond laser is not clearly defined increase in the drilled spot size is verified by experiments and justified by Gaussian distribution of intensity as predicted and discussed earlier in section 2.2. The experimental results shown in the Fig 4.1 were summarized and compared with the theoretical results shown in fig 4.3
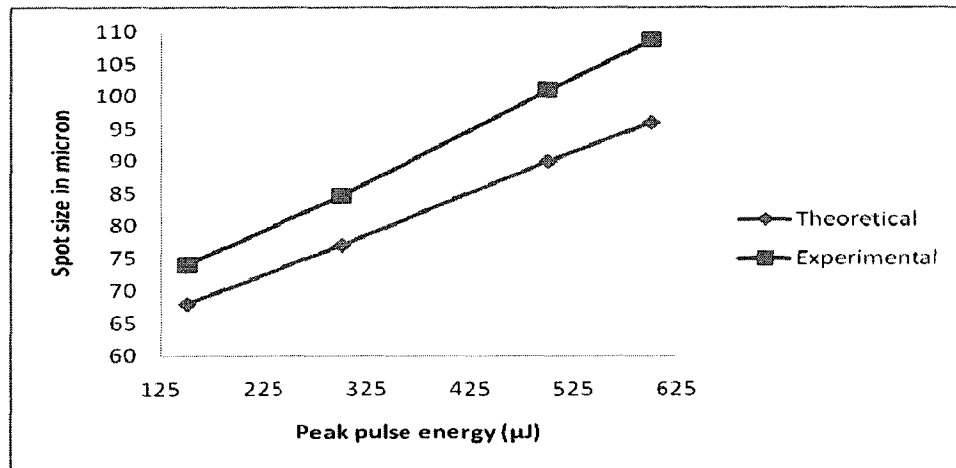
Fig 4.4 *Comparison of experimental and theoretical spot size values with 1064 nm*

wavelength

70

Fig 4.4 shows the comparison of theoretical and experimental value of spot size, x-axis represents the peak pulse energy and y-axis represents the spot size in microns. From fig 4.3 it can be concluded that in nanosecond pulsed laser drilling, the spot size of 1064 nm wavelength vary with the pulse energy while maintaining other parameters constant. The theoretical value is lesser than the experimental values. Difference increases as pulse energy increases. Increase in pulse energy not only increases the spot size, but also increases the heat affected zone. In case of nanosecond laser, since the interaction with the material surface is pyrolythic, material removal is by melting expulsion. In nanosecond laser pulse duration is high, so excess energy is conducted to the surrounding of spot, it starts machining when the material temperature reaches its melting point. Variation in the theoretical and experiments values can be attributed due to conduction.

4.2.2 Influence of laser energy on drilling with 532nm wavelength

Similarly influence of laser energy of 532nm wavelength on drilling was studied with different pulse energies on silicon wafer. All the parameters were same as in the case of 1064nm wavelength, only the pulse energy ranges from 75 μJ to 125 μJ. Pulse energy is lesser as compare to 1064nm wavelength because achieved conversation efficiency of S.H.G was only 20%. However while drilling with 532nm wavelength; the spot size is smaller which increases the intensity per unit area. Also, as discussed earlier, silicon has higher absorption at 532nm. The S.E.M image of silicon sample drilled with 532nm wavelength are shown in fig 4.4

71

(a)

(b)

72
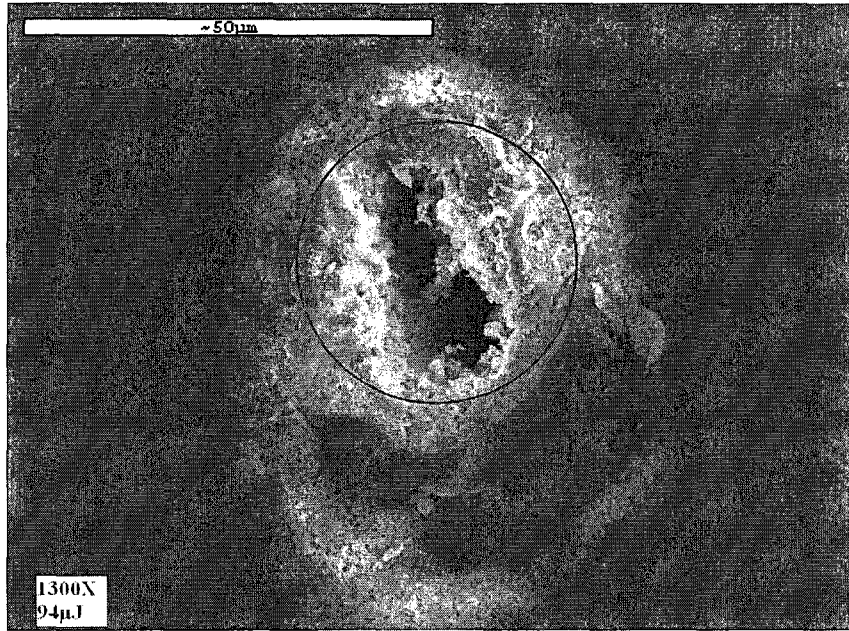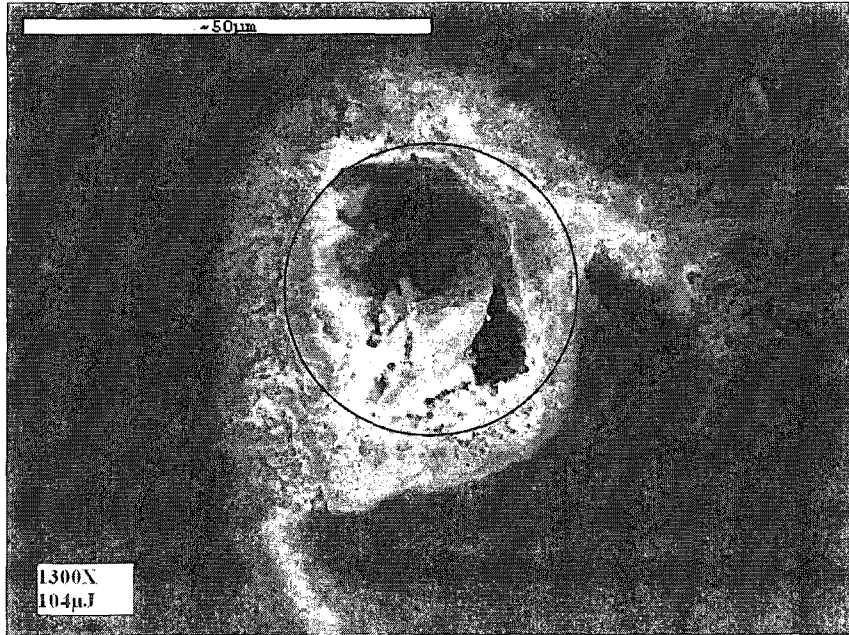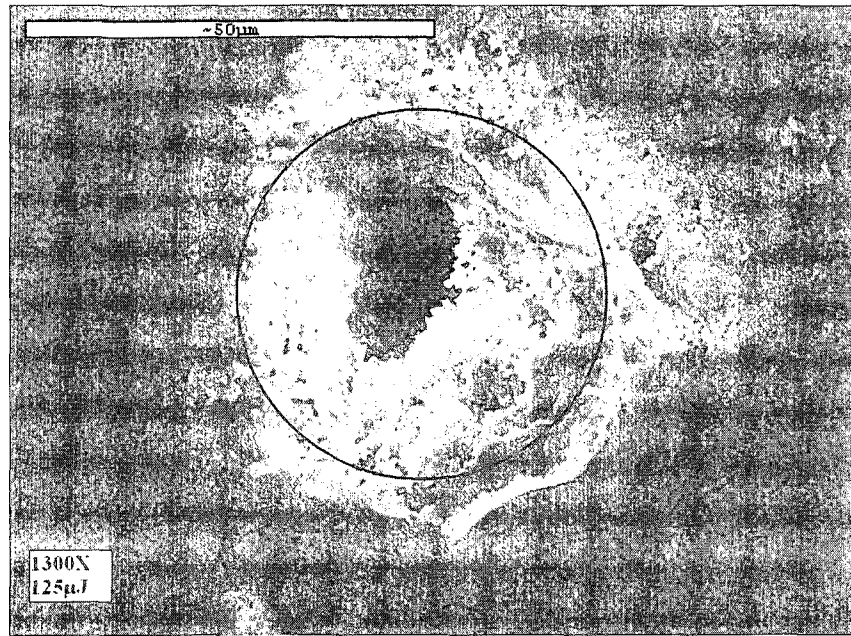
(c)

Fig 4.5 SEM image of different spots drilled with 532 nm for 3 second

From Fig 4.5 it can be observed that with the increase in the pulse energy the spot size increases. As per literature it can be said that silicon absorption for 532nm wavelength is more as compared to 1064nm. As a result of which drilling with 532nm wavelength requires less pulse energy as compared to the 1064nm. The experimental results shown in the Fig 4.5 were compared with the theoretical results in Fig 4.6.
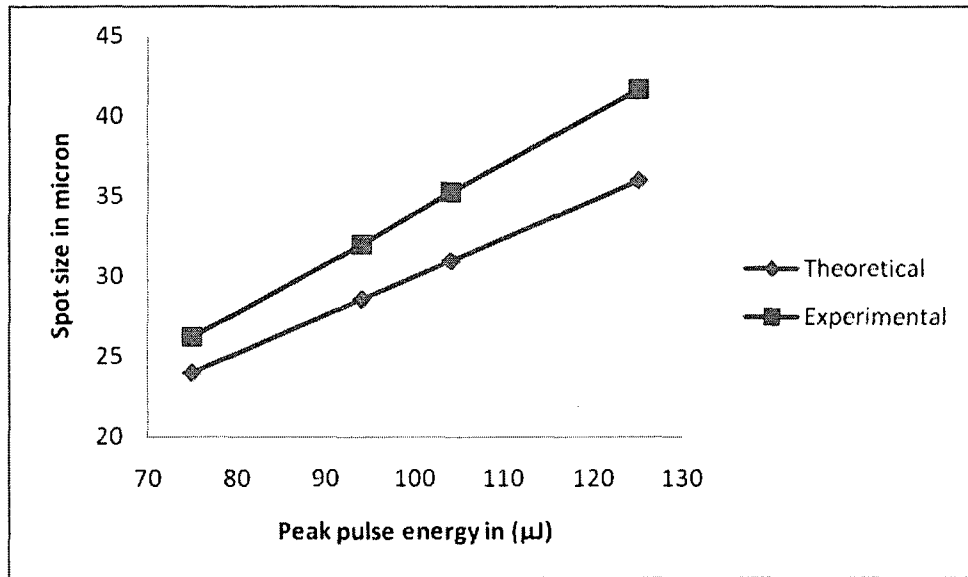
Fig 4.6 *Comparison of experimental and theoretical spot size values of 532nm*

wavelength

Fig. 4.6 shows the comparison of experimental and theoretical spot size value of 532nm wavelength, where x-axis shows peak pulse energy and y-axis shows the spot size in microns. From fig 4.6 it can be concluded that with increase in pulse energy size of the drilled hole also increase which has been explained earlier. From this it is shown that with increase in peak pulse power the difference in theoretical and experimental value increase which is due to conduction losses. Conduction losses increase the top spot size and reduce the bottom spot size. Similarly influence of laser energy with dual frequency is discussed in next section.

4.2.3 Influence of laser energy on drilling with dual frequency

Due to chromatic aberration of plano convex lens both the wavelengths focused at two different foci on the same optical axis as discussed in theoretical modeling. Two different foci increase the depth of focus which increases aspect of ratio. Influence of laser pulse energy on the drilling of silicon with dual frequency wavelengths are shown with S.E.M images in fig 4.6.
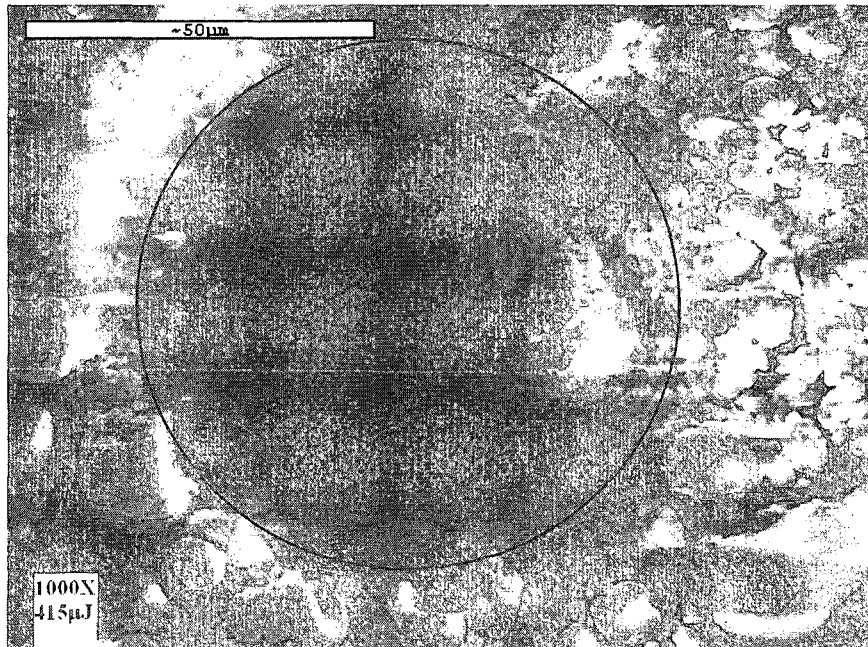
(a)
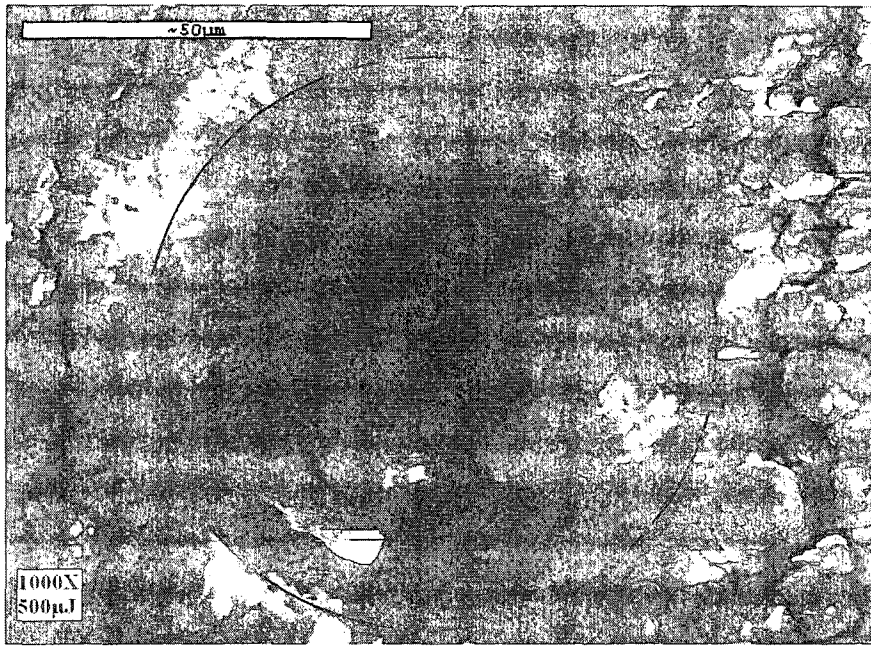
(b)
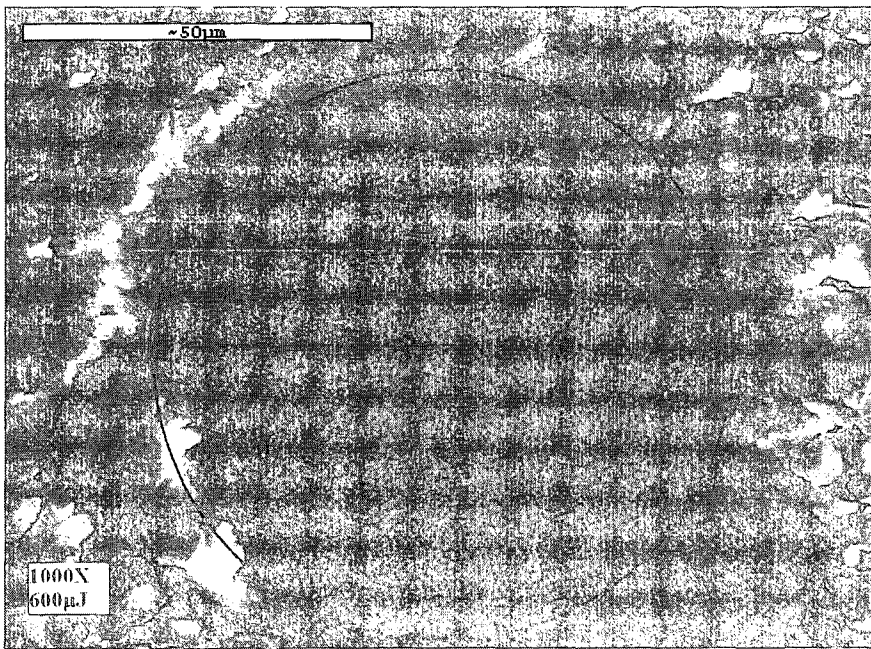
(c)

Fig 4.7 *SEM images of different spots drilled with dual wavelength for 3 second*

From Fig 4.6 it can be observed that size of the drilled spot is smaller as compared to the 1064nm wavelength and bigger than 532nm wavelength. The drilling with dual wavelength is better in terms of the kerf angle, where kerf angle is more with single wavelength as discussed previously. It can also be seen that redopostion of material in dual wavelength drilling as compared to the single wavelength drilling is more on the edges of the spot ablated due to high material removal. This is because the combined effect of both the wavelength has significant effect on energy absorbed. Depth of drilling was increased with dual wavelength due to increase in depth of focus. As smaller wavelength focus exactly on the surface of the silicon, so it will focus the intensity of 532nm wavelength at the surface and 532nm wavelength focused in smaller diameter as compare to 1064nm wavelength, which ultimately increases the aspect ratio of drilling. Fig 4.7 shows the comparison of theoretical and experiment results of drilled spot size with peak pulse power at 20% efficiency of S.H.G.
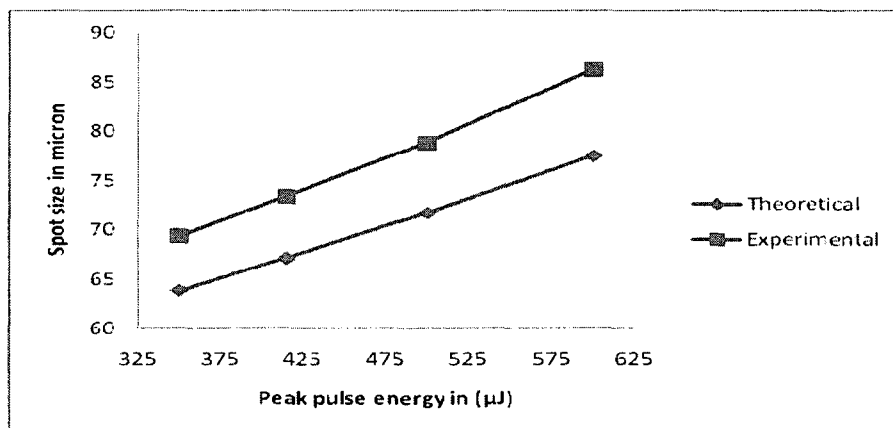
Fig 4.8 *Comparison of experimental and theoretical spot size values of dual wavelength with 20% efficiency*

77

From fig 4.7 it can be shown that even with dual frequency beam spot size will increase with increase in pulse energy. x-axis represent the peak pulse power and y-axis represent spot size, difference in experimental and theoretical value increases with increase in peak pulse power. In nanosecond pulsed laser during drilling with dual wavelength the size of the drilled hole is limited by smaller wavelength whereas the depth of drilling is increased due to the combined effect of dual wavelength which ultimately increases the aspect ratio of the drilling. Efficiency of S.H.G also affects the aspect ratio or the size of the drilling as ratio of the energy of the two wavelengths depends on it; as discussed earlier and explained in theoretical modeling.

4.3 Effect of focal length of lens on spot size

Drilling spot size is directly proportional to the focal length of the lens used, higher the focal length higher the spot size as seen from the mathematical formula (4.2) of spot size.

$$Spot\ size = 2.44\ wavelength * focal\ length/\ Beam\ diameter \qquad (4.2)$$

Focal length of the focusing length not only increases the spot size but also increases the depth of focus of the laser beam. Increase in spot size with focal length reduces the intensity per unity area which increases the demand of energy for same amount of drilling. Experiments were done at two different focusing lenses 25.4 and 50.8 respectively and the S.E.M images of the drilled holes from two different focal length lenses are shown in Fig 4.9.
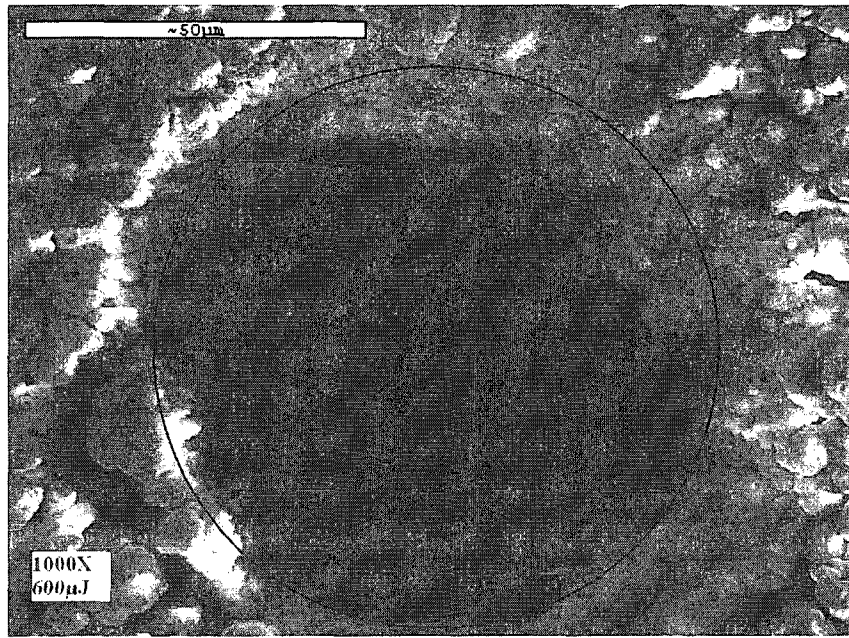
(a)
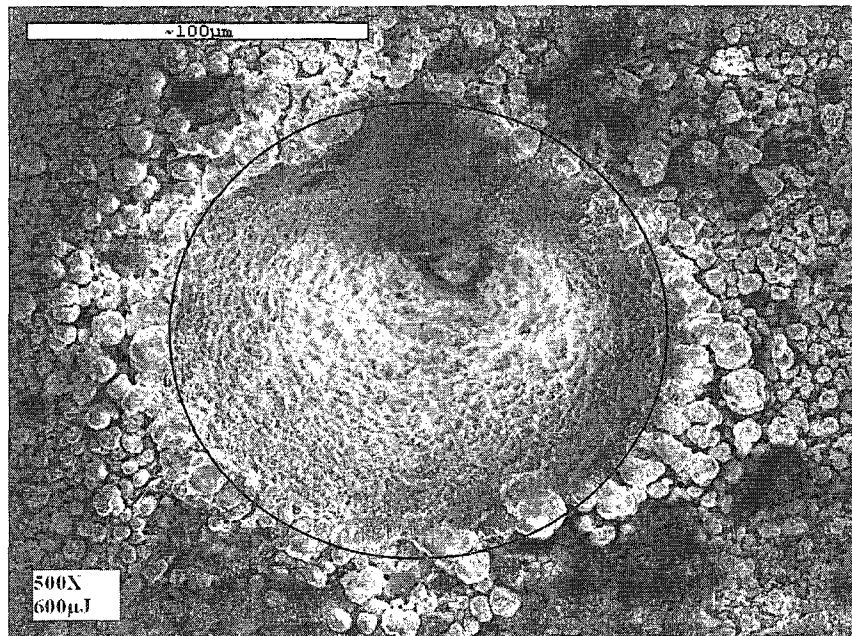
(b)

Fig 4.9 *SEM images of Spot drilled with dual wavelength for 3 second (a) with Fl=*

25.6mm (b) with Fl= 50.8

79

From fig 4.9 it can be concluded that spot size of 50.8 mm focal length is bigger as compared to the spot size of focal length 25.6 mm. Experimental spot size of 50.8 mm focal length is 150 μm with pulse energy of 600 μJ. Similarly spot size of 25.6 mm focal length is 86.27 μm with same pulse energy. This difference in spot size is due to difference in focal point of wavelength are closer to each and 1064nm wavelength having high energy which increases the spot size. And difference in drill depth is due the depth of focus of both the wavelength overlap each other as discussed in chapter 2. This overlap reduces the drilling depth.

4.4 Effect of dual frequency on depth of drilling

Experiments were done with nanosecond pulsed laser having a pulse width of 14ns, with 20% efficiency of S.H.G 1064nm is converted into 532nm wavelength. Beam diameter of the pulsed laser was kept constant at 1.6mm and radius of curvature of the plano convex lens used was 12.9mm. Experiments were done with different pulse energies at a constant repetition rate of 20 kHz by focusing short wavelength focused exactly at the top surface of silicon sample. For each case separate set of experiments were conducted and the results were analyzed with the help of SEM Images are shown in fig.4.10.
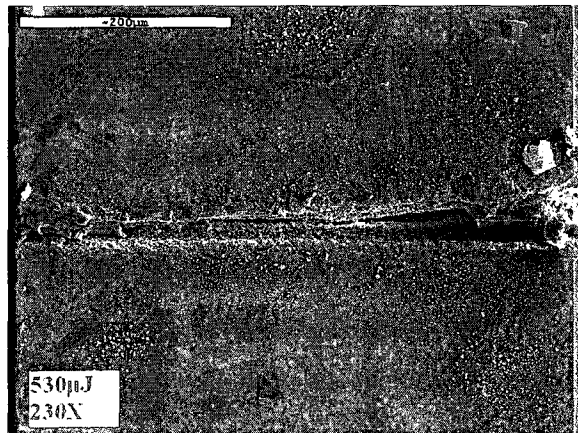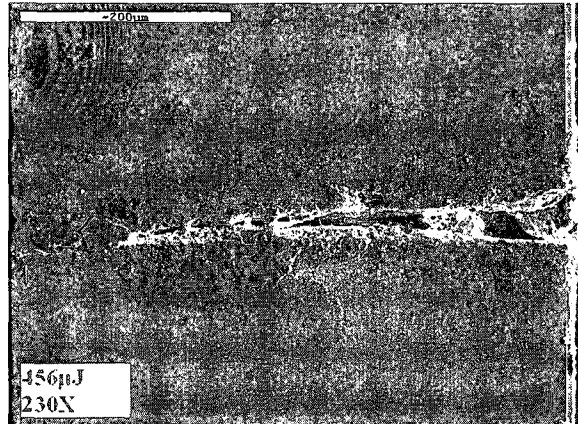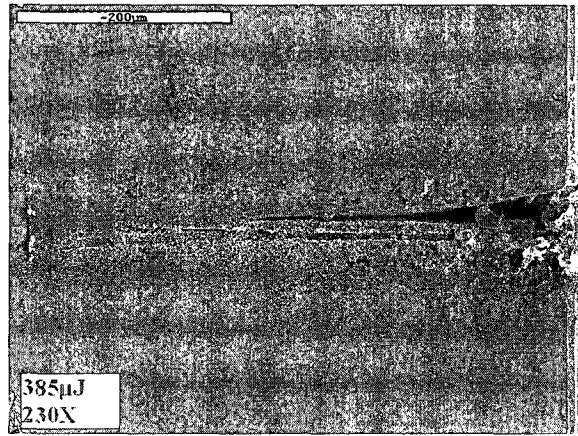
Fig 4.10 *S.E.M images of drilled hole along the depth at different pulse power.*

Fig. 4.10 shows S.E.M images of drilled hole at different pulse powers with constant beam diameter and radius of curvature as discussed earlier. From the fig. it can be observed that with the increase in pulse energy the spot size of drilling was increased and this affect is attributed to change in Gaussian intensity distribution as discussed under the section 2.5. Fig 4.10 shows with increase of pulse energy depth of drilling also increases. At higher pulse powers the kerf angle is less as shown from S.E.M images the bottom spot is bigger in higher pulse energy and smaller in lower pulse energy.
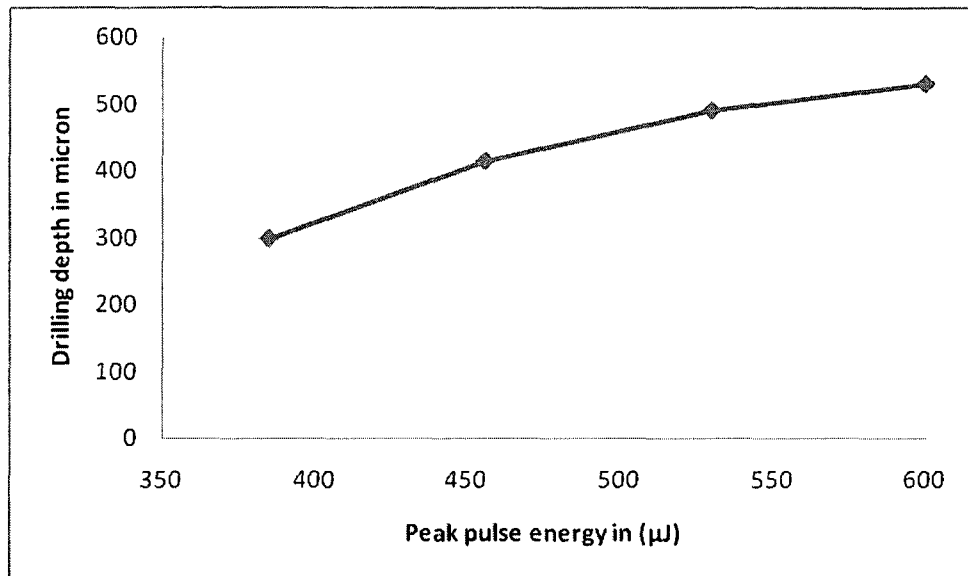
Fig 4.11 *Experimental value of drilling depth of dual frequency drilling.*

Fig.4.11 shows the experimental value of the drilled depth of dual frequency at different pulse power be keeping other parameter kept constant, in fig. y-axis shows the drilling depth in micron and x-axis shows the peak pulse power. From the fig. it can be concluded

that drilling depth is increases with the increase in the pulse energy. But after certain value the ratio of increase in pulse power and drilling depth is reduces. But high pulse power helps in reducing the kerf angle but increase the spot size. Comparison of numerical and experimental value of drill diameter along the drill depth is shown in fig.4.12.
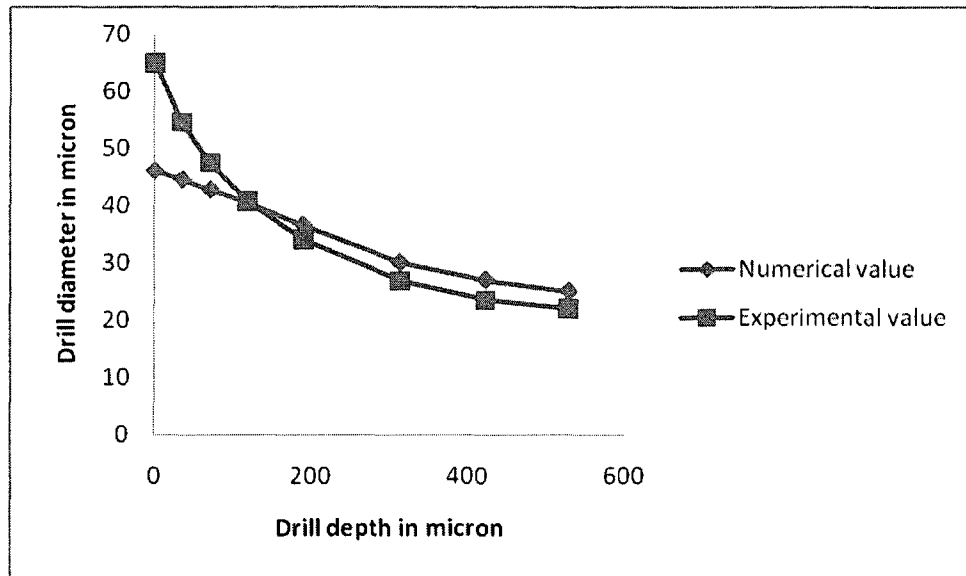
Fig 4.12 *Comparison between numerical and experimental results for 600μJ*

From fig.4.12 it can be concluded that feature size of drilled diameter decreases along the depth of drilling which found to be in good agreement with the corresponding results from the theoretical model. The deviation in the feature size at the surface of the silicon sample is probably due to higher intensity values of 1064nm which was blocked at the surface however during the course of drilling that block intensity heat up the material edges and increases the feature size. Moreover, as seen from fig. 4.10 (c), due to heat

affected zone on the wafer surface the material has chipped which could also influence the measurement. Whereas at the remaining portion experimental values are lower than the theoretical ones. This deviation in experimental value is because exact conduction, convection and radiation losses that are not considered in numerical analysis.

Drilling with dual frequency increase the drilling depth as compare to single wavelength, also the spot size in dual frequency drilling is smaller than the spot size of longer single wavelength. Due to increase in depth and decrease in spot size dual frequency drilling increases the aspect ratio. Dual frequency not only increase the aspect ratio, but also requires less power for drilling, because same power intensity is distributed into two foci to increase the depth of focus. Due to this, intensity distribution along the depth increases while decreasing along the spot size.

4.5 Summary

From the experimental results related to various laser parameters it can be summarized that the quantity and the quality of the laser based drilling with single as well as dual wavelength depends significantly on laser parameters e.g. power, rep. rate and number of pulses hitting the surface. Increase in pulse energy, which can be achieved, either by increasing average power of the laser or by decreasing the rep rate, increases the feature size of the drilling with more amount of heat affected region. From the experimental parts it can be proved that feature size of the drilled hole with dual wavelength remains almost

constant along the drilling depth whereas the same cannot be maintained with single wavelength drilling.

Chapter 5 Conclusion and future work

5.1 Conclusion

Miniaturization of the feature size is the current focus of the research. Shift from continuous laser based micromachining to pulsed laser machining is to reduce the feature size, increase the aspect ratio and to improve the quality of the machining. Different available drilling methods are studied with respect to non laser based as well as laser based techniques. Non laser techniques either involves mechanical methods in which the feature size is limited by the drill bit or it involves time in setting the equipment with slight change in any drill dimensions, tool material also change with respect to the work piece material. On the other hand chemical based methods e.g. ECM, chemical etching, are not clean process so the application are restricted. Some special techniques like LIGA are specifically intended for the MEMS design and require several steps in a sequence manner. Laser based drilling has an additional advantage of non contact drilling which reduce surface damage, there is no need to change the tool only need to change the pulse power according to the damage threshold of the material. Different techniques are available for high aspect ratio drilling, from which laser based dual focus drilling studied to increase the aspect ratio drilling. With the proposed drilling method aspect ratio of the drill hole is increased with minimum optical as well as laser alignment.

In dual focus drilling there are different methods available to focus the laser beam at different foci. Due to limitation of lens replacement with change of dimension in dual focus lens. In optical configuration wavelength specific equipment is required, which not useful for other wavelength, as wavelength is directly proportionate to spot size and laser beam absorption of material is also depends on wavelength, so to change the feature size it is a primary parameter. To change the feature size or with change in work piece material, setup has to modify according to the requirement, which restrict this method for one specific wavelength. From available literature dual frequency drilling is having advantages on over other available drilling methods. Dual frequency drilling method is wavelength sensitive method; feature size can easily modify by changing the beam diameter or by changing the wavelengths. Dual frequency drilling method is studied to increase the aspect ratio with minimum power. Theoretical modeling has been done to predict and compare the drilling of dual wavelength with single wavelength drilling. Modeling has been done separately to optimized the laser as well as optical parameters for high quality dual as well as single wavelength drilling of silicon .Efforts has also been made to select the common focusing lens parameters for drilling with dual wavelength in such a manner that high aspect ratio can be maintain with minimum power. Theoretical modeling has shown that continuity in dual wavelength depends on the radii of curvature of the focusing lens for a particular selection of wavelengths and laser beam diameter. In the case of wavelengths combination of 532nm and 1064nm 12.9mm is the optimum size of the radii of curvature of the lens for 1.6mm laser beam to maintain the continuity.

Dual wavelengths are generated from single laser beam with the help S.H.G crystal, KTP crystal is used for S.H.G., conversion efficiency from fundamental to second harmonic depends on the intensity and polarization of the laser beam incident on the KTP crystal. The optical setup designed for the experiments can be used with minimum optical alignment requirements as it involves few optical components and a single focusing lens was used for focusing both the wavelengths and single wavelength.

Experiments were done in two separate sets, one set of experiments were done with single wavelengths (532nm and 1064nm) drilling with different laser parameters whereas in the second set of experiments dual wavelength was used for drilling and comparing the results with single wavelength drilling. Experiments were done with different pulse energies (75μJ -600μJ) and it was found that with the increase in pulse energy feature size of the drilled hole also increases, whereas on the other hand with increase in rep rate of the laser feature size decreases due to energy of each pulse decreases. These effects were found to same in both types of drilling single as well as dual. For single 532nm wavelength drilling on silicon wafer 106μJ is appropriate pulse power at which there is less affect zone, and for drilling with 1064nm wavelength on silicon with pulse power of 600μJ is appropriate. Drilling with dual wavelength of 532nm and 1064nm laser pulse power of 600μJ and S.H.G efficiency of 20% is appropriate of high depth of silicon wafer drilling. From theoretical modeling it can be concluded that 20% efficiency of S.H.G. appropriate of high depth of drilling as with increase in efficiency S.H.G kerf angle

decreases but depth of drilling decreases. Major advantage associated with dual wavelength drilling is reduction in kerf angle which is high in single wavelength drilling, and aspect ratio of the drilling has also been increased due to intensity distribution over depth of focus of both the wavelengths.

5.2   Future work

In the proposed research project a drilling method based on dual wavelength has been proposed with 532nm and 1064nm. Further work can be done with different set of wavelengths as well as third wavelength can also be involved in the experimental as well as theoretical modeling. Modeling work can also include numerical analysis and incorporate material properties like thermal conductivity to better understand the effect of multi-frequency drilling.

References

[1] S. Charschan, Lasers in Industry, Van Nostrand Reinhold Company, New York, (1972).

[2] B. Narendra, Dahotre, P Sandip, Harimkar, laser Fabrication and Machining of Materials (2008) pp 97-100.

[3] W. S. Rodden, S. S. Kudessia, D. P. Hand, J. D Jones, A Comprehensive study of the long pulse Nd: YAG laser drilling of multi-layer carbon fibre composites'. Optics communications' 210, 319-328 (2002).

[4] J. Kamalu, P. Byrd, A. Pitman, Variable angle drilling of thermal barrier coated nimonic. J Mater. Process. Technol. 122 355-362. (2002)

[5] B. J. Park, Y. J. Choi, C. N. Chu, Prevention of exit crack in micro drilling of soda-lime glass. Ann CIRP 51:347–350 (2002)

[6] A. Smith, "Etching: A Guide to Traditional Techniques", Crowood Press, (2004)

[7] A. J. Van Roosmalen, J. A. G. Baggerman, S. J. H. Brader, "Dry Etching for VLSI", pp 1-4, (1991)

[8] 'http://www.eod.gvsu.edu/eod/manufact/manufact-284.html' September (2008).

[9] K. P. Rajakur, "new developments in electrochemical-machining". keynote papers, annals of CIRP vol 48/2/1999

[10] M. S. Ahmend "the drilling of small deep holes by acid ECM". SME Technical Paper MR-243 (1990)

[11] Mc Geough JA, Advanced methods of machining. Chapmann and Hall (1988)

[12] T. Masuzawa, T. Takawasha, Recent trends in EDM/ECM Technologies in Japan. Keynote paper, Proceedings of the 3rd International Euspen Conference, Eindhoven, vol 1, pp 3–7

[13] S. H. Ahn, S. H. Ryu, D. K. Choi, C. N. Chu, "Electro-chemical micro drilling using ultra short pulses", J. Precision. Engg, 28, 129–134, (2004)

[14] A. Roger, J. Eicher, D. Munchmeyer, R. P. Peters, and J. Mohr. The Liga technique-what are the new opportunities. Journal of Micromechanics and Microengineering, 2(3): 133-140, (1992)

[15] 'http://int.mirl.itri.org.tw/eng/research/micro-electro-mechanical /liga.jsp' Sept (2008)

[16] R. W. Johnstone, M. Parameswaran, an Introduction to Surface-Micromachining pp 34-35 (2004)

[17] M. von Allmen, Laser Beam Interactions with Materials, Springer Series in Materials Science, A. Mooradian and M. Panish, Vol. 2, Springer Verlag, Berlin, (1987)

[18] 'http://www.semrock.com/TechnicalInformation/TN_LaserDamageThreshold/' July (2008)

[19] P. P. Pronko, S. K. Dutta, J. Squier, J. V. Rudd, D. Du, and Mourou, "Machining of sub-micron holes using a femtosecond laser at 800nm," Optics Communications, 114, 106-110 (1995)

[20] B. N. Chichkov, C. Momma, S. V. Nolte, F. Alvensleben, and A. Tunnermann, "Femtosecond, Picosecond and Nanosecond laser ablation of solid," Applied Physics, A 63, 109-115 (1996)

[21] A. Kurela et al., review paper Journal of Biomaterial applications Vol. 20 July, (2005).

[22] P. Christel, A. Meunier, and J. M. Dorlot, "Biomechanical compatibility and Design of Ceramic Implants for orthopedic surgery", Ann. N.Y. Acad. Sci., 523: 234-256 (1988)

[23]   'http://www.imperial.ac.uk/research/photonics/research/topics/ablate/index.htm' July (2008)

[24] X. Liu, "Submicron lines in thin metallic films micromachined by an ultrafast laser oscillator," technical digest-conference on lasers and electro-optics, 511, (1998)

[25] 'http://www.cmxr.com/micromachining/handbook' January (2008)

[26] A. Borowiec, H. K. Haugen, "Morphological and chemical evolution on InP (100) surface irradiated with femtosecond laser" Appl. Phys. Lett. 82, 4462 (2003)

[27] T. H. R. Crawford, A. Borowiec, H. K. Haugen, CLEO/IQEC and PhAST 2004 Technical Digest on CD-ROM, The optical society of America, Washington, DC, CtuP40. (2004).

[28] T. Q. Jia, H. X. Chen, M. Huang, F. L. Zhao, J. R. Qiu, R. X. LI, Z. Z. Xu, X. K. He, J. Zhang, H. Kuroda, "Formation of nanogratings on the surface of a ZnSe crystal irradiated by femtosecond laser pulses" Phys. Rev B 72, 125429 (2005).

[29] Mark J. Jackson et al., Microfabrication and Nanomanufacturing pp. 245-250.

[30] C. Körner, R. Mayerhofer, M. Hartmann and H. Bergmann, Physical and material aspects in using visible laser pulses of nanosecond duration for ablation, Appl. Phys. A, 63, pp. 123-131, (1996)

[31] M. R. H. Knowles, "Micro-machining of metals, ceramics and polymers using nanosecond lasers", Int. J. Adv. Manuf. Technol. 33, 95-102 (2007).

[32] A. Oestendorf, G. Kamlage, F. Klug, B. N. Chickkov "femtosecond versus picosecond laser ablation" In: Proceedings of the SPIE conference, Photon processing in microelectronic and photonic IV, San Jose, California, vol 5713, pp1-8 (2005).

[33] D. Karanaksi, M. Knowles, K. Alty, M. Schalf, H. Snelling (2005) "Comparison of glass processing using high repetition femtosecond (800nm) and UV (255nm) nanosecond pulsed lasers". In proceedings of the SPIE conference, Microfluidics,

BioMEMS and Medical Microsystems III, San Jose, California, vol. 5718, pp 216-277 (2005).

[34] D. Breitling, A. Ruf, F. Dausinger. "Fundamental aspects in machining of metals with short and ultra short laser pulses". In proceeding of the SPIE conference, Photon Processing in Microelectronics and Photonic III, San Jose, California, vol. 5339, pp 49-63 (2004)

[35] A. Schoonderbeek, C.A. Biesheuvel, R. M. Hofstra, K. J. Boller, J. Meijer. "The influence of the pulse length on the drilling of metals with an excimer laser". Journal of laser applications 16:85-91 (2004).

[36] K. T. Voisey, S. S. Kudesia, W. S. Rodden, D. P. Hand, J. D. Jones, T. W. Clyne, Melt ejection during laser drilling of metals, Materials science and engineering, A 356, 414-424 (2003)

[37] K. Verhoeven, "Modelling Laser Percussion Drilling" (2004).

[38] J. C. Verhoven, J. K. Jansen, R. M. Mattheij, Modeling laser induced melting mathematical and computer modelling 37, 419-437 (2003)

[39] D Elza, G. White, laser beam machining. In: Davis JR(ed) ASM Handbook: machining, ASM international, Ohio, vol.16, pp 572-578 (1989)

[40] P. Hariharan, Basic of interferometry, Academic Press, pp15-20, 1992

[41] B. K. A. Ngoi "Sub-microdrilling with ultrafast pulse laser interference" Appl. Phys. B 79, 99–102 (2004)

[42] 'http://www.ulooptics.com/ulo_optics/index.asp' August (2008).

[43] B. Tan, K. Venkatakrishnan, Dual-focus laser micro-machining, Journal of modern Optics, Vol. 52,No. 17, 2603-2611, 2005

[44] B. Tan, K. Venkatkrishnan, N. R. Sivakumar and G. K. Gan. "Laser drilling of thick material using femtosecond pulse with a focus of dual-frequency beam" Opt. Laser Technol. 35, 199-202 (2003)

[45] M. Van Elsena, M. Baelmansa, P. Mercelisa and J. P. Kruth. "Solutions for modeling moving heat sources in a semi-infinite medium and applications to laser material processing". Int. J. Heat Mass transfer. 50, 4872 - 4882 (2007)

[46] N. Bloembergen, Encounters in Nonlinear Optics: Selected Papers of Nicolaas Bloembergen (With Commentary), World Scientific, 1997

[47] 'http://www.cvilaser.com/Catalog/Pages/Template2.aspx?pcid=155' April (2008)

[48] Melles Griot optics guide.

[49] 'Virginia Semiconductor, Inc. www.vriginiasemi.com' July (2008)

[50] 'http://www.u-oplaz.com/crystals/crystals20-1.htm' August (2008)

[51] Robert W. Boyd, Nonlinear optics 3rd edition (2008)

[52] 'http://en.wikipedia.org/wiki/Frequency_doubling' Sept (2008).

[53] Principle of physical optics / C. A. Bennett.

[54] N. Subrahmanyam, Brij lal, M.N. Avadhanulu, Optics, (2006)

[55] R. F. Belt, G. Gashurov, and Y.S. Liu, "KTP as a harmonic generator for Nd:YAG lasers," laser Focus 21, 110 (1985).

[56] F. C. Zumsteg, J. D. Bierlein, and T. E. Gier, "$K_xRb_{1-x}TiOPO4$: a new nonlinear optical material," J. Appl. Phys. 47, 4980 (1976).

[57] J. Q. Yao and T. S. Fahlen, "Calculations of optimum phase match parameters for the biaxial crystal $KTiOPO_4$," J. Appl. Phys. 55, 65 (1984).

[58] Y. S. liu, L. Drafall, D. Dentz, and R. Belt, "Nonlinear optical phase-matching properties of $KTiOPO_4$," Technical information series Rep. 82CRD016 (1982).

[59] D. T. Hon, "High average power, efficient second harmonic generation," in laser Handbook, M.L. Stitch, ed. Vol.3, p.421. (1979).

[60] Y. S. Liu, D. Dentz, and R. Belt, "High average power intracavity second harmonic generation using KTiOPO4 in an acousto-optically Q-switched Nd:YAG laser oscillator at 5 kHz," Opt. Lett. 9, 76 (1984).

[61] P. E. Perkins, and T. S. Fahlen, "20-W average power KTP intracavity doubled Nd:YAG laser," J. Opt. Soc. Am. B 4, 1066 (1987).

[62] Fujian Castech Crystal, Inc. catalogue, crystals (1996).

[63] W. Koechnev, Solid State laser Engineering, spring-Verlag, Berlin (1992).

[64] "http://www.britannica.com/EBchecked/topic/463171/plano-convex-lens" Sept (2008)

[65] "http://en.wikipedia.org/wiki/Image:Gaussianbeam.png" August (2008)

[66] K. Salonitis, A. Stournaras, G. Tsoukantas, P. Stavropoulos and G. Chryssolouris, "A theoretical and experimental investigation on limitations of pulsed laser drilling". J. Mater. Process. Technol.183, 96-103 (2007)